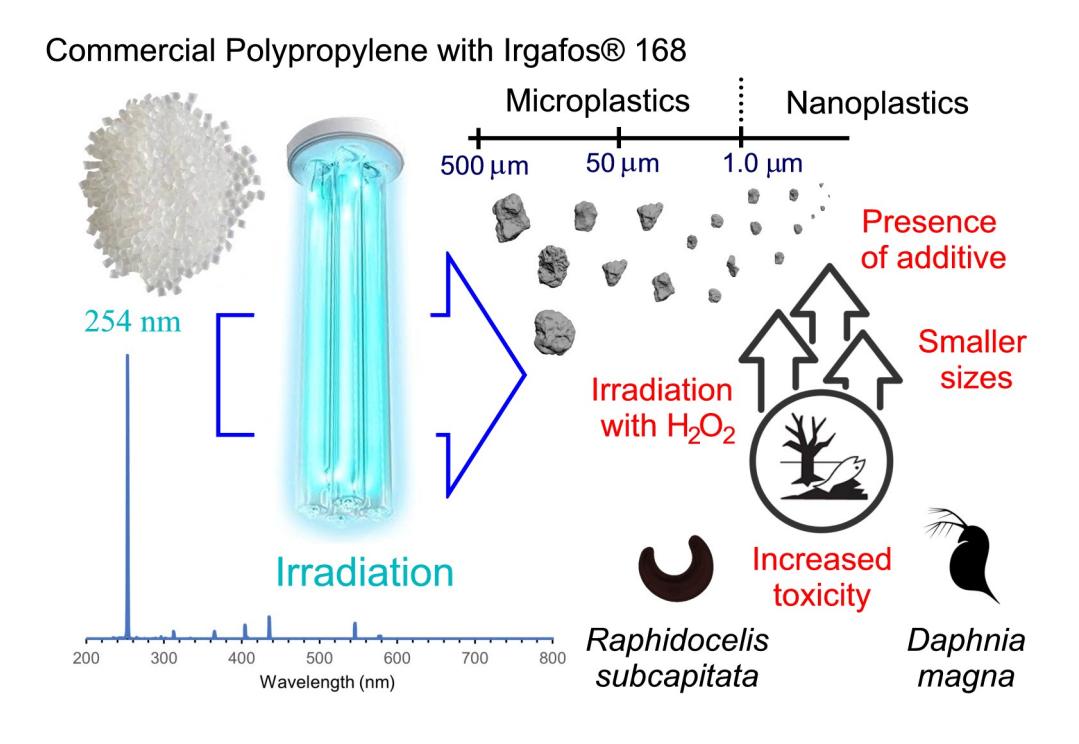
Aquatic toxicity of UV-irradiated commercial polypropylene plastic particles and associated chemicals

This manuscript version is made available in fulfillment of publisher's policy. Please, cite as follows:

Laura Contreras-Castillo, Enrique Blázquez-Blázquez, María L. Cerrada, Georgiana Amariei, Roberto Rosal. Aquatic toxicity of UV-irradiated commercial polypropylene plastic particles and associated chemicals. Journal of Hazardous Materials 494, 138645, 2025

https://doi.org/10.1016/j.jhazmat.2025.138645



Aquatic toxicity of UV-irradiated commercial polypropylene plastic particles and associated chemicals

Laura Contreras-Castillo 1 , Enrique Blázquez-Blázquez 2 , María L. Cerrada 2 , Georgiana Amariei 1,* , Roberto Rosal 1

¹Department of Chemical Engineering, Universidad de Alcalá, E-28871 Alcalá de Henares, Madrid, Spain ²Instituto de Ciencia y Tecnología de Polímeros (ICTP-CSIC), Juan de la Cierva 3, Madrid 28006, Spain

Abstract

Plastics often contain non-polar chemical additives, such as antioxidants, flame retardants, plasticizers, and UV stabilizers, which improve performance but have poorly understood environmental risks. This study assessed the aquatic toxicity of polypropylene (PP) containing the antioxidant Irgafos 168 (IRG) to the crustacean Daphnia magna and the green alga Raphidocelis subcapitata. Commercial PP containing IRG (PPc) and additive and oligomer-free PP (PPd) were irradiated at 254 nm using germicidal light, both with and without H₂O₂. The tested particles included microplastics (MPs, 1-50 μm and 50-500 μm) and nanoplastics (NPs, < 1 μm). The results showed that the toxicity was influenced by particle size, concentration, and the presence of the antioxidant additive. Smaller particles, along with the presence of IRG and its degradation products, tris(2,4-ditert-butylphenyl) phosphate, bis(2,4-di-tert-butylphenyl) phosphate, and 2,4-di-tert-butylphenol, contributed to higher toxicity in both D. magna and R. subcapitata. The highest toxicity was observed for NPs containing IRG (PPc), which resulted in an EC₂₀ for D. magna immobilization of 7.2 ± 0.1 mg/L, compared to the less toxic NPs free of IRG (EC₂₀ 28.7 \pm 4.2 mg/L). The growth rate of R. subcapitata was also more affected by NPs generated from PPc (EC₂₀ 0.2 ± 1.2 mg/L) than by the corresponding NPs free of IRG (LOEC 3 mg/L). Our findings showed that the main toxicity was driver was an increase of intracellular reactive oxygen species, lipid peroxidation (LPO), damage to cell membrane integrity and impairment of esterase activity. The results demonstrated that irradiated plastic particles act as carriers for toxic non-polar compounds, enhancing negative effects on aquatic organisms, with particle size being a key factor. This study highlights the complex toxicological impacts of micro- and nano-plastics containing additives on aquatic biota.

1. Introduction

Plastic pollution has become a major environmental issue with serious implications for ecosystems, food safety, and human health. Plastics, particularly microplastics (MP), are pervasive in terrestrial, freshwater, and marine environments. They are durable and break down slowly, accumulating in water bodies, soil, and other compartments. The reason is the low circularity of their lifecycle and their persistence, which allows plastics to spread across ecosystems, entering food webs and potentially affecting wildlife and human populations [7]. Most MPs result from the breakdown of larger plastic items, such as packaging materials, tyre abrasion, and the wearing of synthetic textiles when exposed to mechanical stress and photochemical degradation [2], [38]. Plastic fragmentation proceeds to smaller and smaller sizes eventually producing particles with sizes below

 $1~\mu m$, which are typically referred to as nanoplastics (NPs) [10]. MPs and NPs are concerning due to their ability to move up the food chain, carrying associated chemicals and ultimately reaching humans through contaminated seafood, meat, or other products [24].

Plastics may contain a high number of chemical additives, such as antioxidants, flame retardants, plasticizers, and UV stabilizers, which enhance performance and durability [43]. The release of additives through plastic degradation accelerates upon plastic fragmentation and poses significant environmental and health risks [44]. Many of these additives fall under the ECHA's category of persistent, bioaccumulative, and toxic chemicals. Many others remain insufficiently studied in terms of their ecological impact [23]. Besides, these chemicals become subject to additional degradation and transformation processes that can make them more hydrophilic and mobile through the sediment and water column [9]. Additives may degrade during use giving rise to a variety of known compounds such as the quinoid derivatives phenolic antioxidants [27]. However, the degradation of additives under environmental stressors remains significantly understudied. This gap includes the

^{*} Corresponding author: georgiana.amariei@uah.es Version of Record May 17, 2025

photochemical degradation under solar irradiation, biological transformation, and alterations induced by industrial processes, including UVC irradiation used in water treatment.

Irgafos 168, tris(2,4-di-tert-butylphenyl) phosphite, hereafter referred to as IRG, is a processing stabilizer that acts as a secondary antioxidant. It specifically targets the hydroperoxides produced through the auto-oxidation of polymers, preventing processinduced degradation and enhancing the performance of primary antioxidants, which is necessary to increase the durability and stability of the polymer during processing. IRG has been associated to potential neurotoxicity due to the release of phosphatecontaining degradation species, mainly its oxidized form, tris(2,4-di-tert-butylphenyl) phosphate [15]. The concern is supported by the well-known fact that organophosphate chemicals have been shown to inhibit acetylcholinesterase, leading to disruptions in normal nervous system function [42]. There is some evidence that neurotoxicity concerns may have been overestimated, at least due to dietary exposure [28]. However, the effect to environmental organisms to IRG and its degradation products is largely unknown because of the low water solubility of IRG (< 5 μg/L at 20 °C), which makes it difficult to perform conventional aquatic toxicity assays.

Recent evidence of the aquatic toxicity of IRG has been obtained by using additive-free nanoplastics as carriers for the insoluble phosphite additive, indicating toxicity near or even below its solubility limit [37]. However, there is still no clear data on the toxicity of IRG degradation products. In this work, we tested the toxicity of polypropylene (PP) micro- and nanoplastics with and without its commercial additive IRG and the PP oligomers (PPO) to the green alga Raphidocelis subcapitata and the freshwater cladoceran Daphnia magna. Our results demonstrated that NPs generated in a top-down approach via irradiation of commercial PP can act as carriers for toxic non-polar compounds, including the antioxidant additive IRG and its transformation products. We also showed that the generation of small particles in the NP range $(< 1 \mu m)$ are the main cause for toxicity, triggered by an increase of intracellular reactive oxygen species (ROS) followed by lipid peroxidation (LPO), damage to cell membrane integrity and impairment of esterase activity.

2. Materials and methods

2.1. Plastic materials and chemicals

Pellets of commercial metallocene-catalysed isotactic polypropylene (PPc) measuring 4 ± 1 mm in size,

clear in colour, with a molecular weight of 250,000 g/mol, and containing 0.037 wt% of the antioxidant additive Irgafos 168 (IRG) and 0.2 wt% polypropylene oligomers (PPO), were obtained from LyondellBasell (Rotterdam, Netherlands). Additive-free PP (PPd) pellets and an extract (EXT) containing the additive (IRG) and oligomers (PPO) were obtained through Soxhlet extraction in dichloromethane (DCM) for 8 h from mechanically ground PPc pellets [6]. The oligomers were separated from the additive by elution with hexane using a silica column activated for 24 h at 150 °C as described elsewhere [37].

Irgafos 168 (tris(2,4-di-tert-butylphenyl)phosphite, $[(C_4H_9)_2C_6H_3O]_3P$, CAS: 31570-04-4) was purchased from Sigma-Aldrich. Dichloromethane (DCM, CH₂Cl₂, CAS number: 75-09-2, Multisolvent HPLC grade) was acquired from Scharlab (Spain). Hydrogen peroxide (H2O2, CAS number: 7722-84-1, 35 wt%) was acquired from PanReac AppliChem-ITW Reagents. Sodium sulphite (Na₂SO₃, CAS number: 7757-83-7) was obtained from Sigma-Aldrich. 2',7'-dichlorodihydrofluorescein diacetate (H₂DCFDA, CAS number: 4091-99-0) and fluorescein diacetate (FDA, CAS number: 596-09-8) were purchased from Sigma-Aldrich. Propidium iodide (PI, CAS number: 25535-16-4) was obtained from Sigma Aldrich. C4-BODIPY and Qubit Protein Assay Kit (Invitrogen) were acquired from Thermo Fisher Scientific. The ultrapure water used was generated with a Direct-QTM 5 Ultrapure Water System from Millipore with resistivity > 18 $M\Omega$ cm at 25 °C (Bedford, MA, USA).

2.2. Ultraviolet irradiation treatments

Plastic particles of commercial polypropylene (PPc-MPs) and additive-free polypropylene (PPd-MPs), with sizes in the 100-500 µm range, were obtained by mechanical grinding plastic pellets in a blender, using liquid nitrogen to make them brittle. PPc-MPs (100-500 µm, 0.037 wt% IRG, 0.2 wt% oligomers) and PPd-MPs (100-500 μm) were suspended in ultrapure water (10 g/L), with and without the addition of 15 mg/L of H₂O₂ (35 wt%) and irradiated for 10 min using a 15 W Heraeus Noblelight TNN 15/32 low pressure mercury vapour lamp (UV) emitting at 254 nm, in a 1 L cylindrical borosilicate reactor (17×9 cm) under magnetic stirring at 50 rpm. The irradiance at the central point of the reactor was 14.2 mW cm⁻². The emission spectrum of the 254 nm UV lamp used for the irradiation experiments is presented in Figure S1 of the Supporting Material (SM). The irradiated materials were vacuum filtered through a 50 µm stainless steel meshes and a 1 µm glass microfiber filters (Whatman). With this procedure, the following irradiated particles were prepared:

- i) PPc 50–500 μm with and without H_2O_2 treatment (PPc-50–500 and PPc-50–500+ H_2O_2).
- ii) PPd 50–500 μ m with and without H₂O₂ treatment (PPd-50–500 and PPd-50–500+H₂O₂).
- iii) PPc 1–50 μ m with and without H₂O₂ treatment (PPc-1–50 and PPc-1–50+H₂O₂).
- iv) PPd 1–50 μ m with and without H_2O_2 treatment (PPd-1–50 and PPc-1–50+ H_2O_2).
- v) PPc nanoplastics, $< 1 \mu m$, with and without H_2O_2 treatment (PPc-NP, PPc-NP+ H_2O_2).
- vi) PPd nanoplastics, $< 1 \mu m$, with and without H_2O_2 treatment (PPd-NP, PPd-NP+ H_2O_2).

As control experiments IRG, PPO and EXT were irradiated in the absence of the plastic particles with the purpose of clarifying the toxicological effects of the individual components of the commercial PP material. Besides, PPd-NP and PPd+H₂O₂ were re-additivated with the same amount of IRG, PPO and EXT in the commercial plastic, thereby producing the following materials: PPd-NP+EXT; PPd-NP+PPO; PPd-NP+IRG) and PPc-NP+H₂O₂ (PPd-NP+EXT+H₂O₂; PPd-NP+PPO+H₂O₂; PPd-NP+IRG+H₂O₂), without and with H₂O₂ treatment respectively. The possible excess of H₂O₂ in the aqueous solutions was removed using sodium sulfite as explained elsewhere [21].

2.3. Analyses

The total organic carbon (TOC) for particle suspensions < 1 μm was measured using a Multi N/C 3100 Series TOC-/TNb analyzer (Analytic Jena) and the result was used to calculate the exposure to plastic particles in mass concentration units. The concentration of larger particles was determined by mass measurement. The particle size distribution of MP fractions in the 1-50 µm and 50-500 µm size ranges was determined using optical microscopy. MP samples suspended in ultrapure water at a concentration of 50 mg/L were placed on a glass plate, and images were captured in Bright Field mode with a Nikon Eclipse E200 microscope equipped with a Micros Copia Digital camera. The images were subsequently processed with ImageJ software to determine the size distribution and median particle size was reported. The surface morphology of MPs was assessed using a field emission Scanning Electron Microscope (SEM), Jeol JSM-IT500, operating at 25 kV on gold-sputtered samples. The particle size distribution of NP suspensions, at a concentration of 50 g/L, was measured by Dynamic Light Scattering (DLS) using a Malvern Zetasizer Nano ZS apparatus. The ζ -potential of NPs

was determined in the same apparatus by means of electrophoretic light scattering. The results of particle size and ζ -potential (NPs) for the materials used in this work is shown in Table 1.

The characterization of chemical changes in the polymer particles and the extraction products was performed by Fourier transform infrared spectroscopy (FTIR) using a total attenuated reflectance device (ATR-FTIR, Thermo Scientific Nicolet iS20 FTIR Spectrometer). The spectra were recorded in the 650-4000 cm⁻¹ range with a resolution of 4 cm⁻¹ in 64 scans.

The analytical determination of additives from both non-irradiated and UV-generated plastic particles (with and without $\rm H_2O_2$) was performed using Gas Chromatography-Mass Spectrometry (GC-MS). This system consisted of a Hewlett Packard 6890 gas chromatograph coupled with an Agilent Technologies 5973 mass spectrometer. Analyte separation was conducted on a DB5-HT capillary column (15 m length, 250 µm internal diameter, 0.1 µm film thickness). Helium was used as the carrier gas, maintained at a constant flow rate of 1 mL/min. The mass spectrometer operated in electron ionization mode with an ionization energy of 70 eV. The optimal chromatographic protocol was established based on previous research [6].

2.4. Toxicity tests

Toxicity bioassays with cladoceran crustacean Daphnia magna (MicroBioTests, Belgium) was performed following the OECD Test Guideline 202 [35] and the ISO Standard 6341 [17]. Briefly, the dormant eggs were first hatched in nutritive medium, at 20 ± 1 °C, under continuous side illumination of 6000 lux for 72 h. The exposure experiments were set up in plates containing 5 neonates and 5 mL culture medium, either without added plastic particles (control) or supplemented with predefined concentrations of plastic particles. Each condition was tested in triplicate. All experiments were conducted in darkness at 20 \pm 1 °C. The plastic particles were tested in a concentration range of 1-50 mg/L. The endpoint for acute toxicity was the immobilization of daphnids with respect to the controls over a 48 h incubation period. Micrographs of daphnids after 48 h incubation period were captured in Bright Field mode with a Nikon Eclipse E200 optical microscope equipped with a Micros Copia Digital camera.

Toxicity bioassays with the green alga *Raphidocelis subcapitata* algae (MicroBioTests, Belgium) were performed following the OECD Test Guideline 201 [34] and the ISO Standard 8692 [18]. In short, exposure experiments were conducted in triplicate in transparent 24-well plates each containing

Table 1. Characterization the plastic particles used in this work.

Material	Sample	Particle size ^a	ζ -potential a
	PPc-50-500	143 ± 9 μm	-
	$PPc-50-500+H_2O_2$	$86 \pm 5 \mu m$	-
PPc	PPc-1-50	$33 \pm 3 \mu m$	-
rrc	$PPc-1-50+H_2O_2$	$35 \pm 1 \mu m$	-
	PPc-NP	$383 \pm 93 \text{ nm}$	-15.2 ± 7.3 mV at pH 9.9
	PPc-NP+H ₂ O ₂	$246 \pm 21 \text{ nm}$	-15.1 ± 5.1 mV at pH 7.1
	PPd 50-500	$86 \pm 4 \mu m$	-
	$PPd-50-500+H_2O_2$	$56 \pm 13 \mu m$	-
PPd	PPd-1-50	$18 \pm 1 \mu m$	-
rru	$PPd-1-50+H_2O_2$	$23 \pm 2 \mu m$	-
	PPd-NP	$208 \pm 53 \text{ nm}$	-25.5 ± 5.5 mV at pH 5.3
	PPd-NP+H ₂ O ₂	$223 \pm 24 \text{ nm}$	$-22.0 \pm 4.4 \text{ mV}$ at pH 5.6

^a Measured at a concentration of 50 mg/L of particle suspensions. PPc: commercial PP (containing 0.037 wt% IRG and 0.2 wt% PPO), PPd: additive-free PP, 50-500: MPs within 50-500 μm size range generated without H_2O_2 ; 50-500+ H_2O_2 : MPs within 50-500 μm size range generated with H_2O_2 ; 1-50: MPs within 1-50 μm size range generated without H_2O_2 ; 1-50+ H_2O_2 : MPs within 1-50 μm size range generated with H_2O_2 ; NP: NPs (< 1 μm) generated without H_2O_2 ; NP+ H_2O_2 : NPs (< 1 μm) generated with H_2O_2 . The intervals (±) denote standard deviation.

10⁶ cells/mL in culture medium. All experiments were conducted at 23 ± 1 °C under continuous illumination of 6000 lux. Algal growth was assessed in the presence of plastic particles at concentrations ranging from 1 to 50 mg/L by measuring chlorophyll autofluorescence (450-672 nm) over a 72 h incubation period using a Fluoroskan Ascent FL fluorimeter. In addition, micrographs of algae after 72 h incubation were recorded with a Leica TCS SP5 laser scanning confocal microscope in Bright Field mode and at Chl autofluorescence channel ($\lambda_{ex.}$ 488/595, $\lambda_{em.}$ 700 nm). Abiotic incubation experiments (in absence of algae) were set up for the MP fractions and turbidity of each concentration was measured with a portable turbidimeter (Orbeco-Hellige, Model 966) to track the particle aggregation.

For effect calculations, the median effect equation was used [8]:

$$\frac{f_a}{1 - f_a} = \left(\frac{c}{EC_{50}}\right)^m \tag{1}$$

Where c represents the concentration of a substance that causes damage to a fraction f_a of the population (inhibition), EC_{50} is the median effective concentration and m is a parameter that characterizes the shape of the dose-response curve. The EC_{20} , defined as the concentration causing 20% damage, was calculated using the median effect equation with fa set to 0.2 and is expressed in mg/L with its corresponding 95% confidence intervals. All statistical analyses were performed in R, with ANOVA and ANCOVA implemented using the aov() function followed by Tukey's HSD pot-hoc test for pairwise comparison [36]. When it was not possible

to use the median effect equation due to a lack of normality/non-monotonic dose-effect relationships, the significant effect, defined as the lowest observed effect concentration (LOEC), was determined using the non-parametric Mann-Whitney-Wilcoxon test (p > 0.05).

Key physiological parameters related to toxicity responses were assessed by using appropriate fluorochromes that allow for the detection of specific cellular alterations. Intracellular reactive oxygen species (ROS) in R. subcapitata were assessed after exposure to MPs and NPs using H₂DCFDA (1 mM in ultrapure water, 30 min incubation, excitation/emission wavelengths 485/528 nm) in microplate reader. Membrane integrity, and non-specific esterase activity, were also assessed in R. subcapitata after exposure to MPs and NPs. The fluorescent dyes used to evaluate these parameters were propidium iodide (PI) for membrane integrity (50 µg/mL in ultrapure water, 10 min incubation, excitation/emission wavelengths 535/617 nm), and fluorescein diacetate (FDA) for metabolic activity (25 µg/mL in ultrapure water, 30 min incubation, excitation/emission wavelengths 485/528 nm). Membrane lipid peroxidation (LPO) was tracked using C4-BODIPY, a key indicator of oxidative damage and cell toxicity. This dye shifts its fluorescence from when it reacts with lipid radicals, allowing dynamic monitoring of oxidative stress in live cells. C4-BODIPY was used at 50 µM in ultrapure water after 30 min incubation with excitation/emission wavelengths 485/528 nm. For all the four assays algae suspensions (180 μ L) were incubated with 20 μ L of fluorescent dye in 96-well black microplates at room

temperature in the dark, with each sample tested in triplicate. Fluorescence for ROS, PI, FDA, and C4-BODIPY was recorded using a Fluoroskan Ascent FL microplate reader, and results were normalized to in vivo Chl a autofluorescence. For ROS visualization, fluorescence was also recorded by confocal microscopy.

In the case of *D. magna*, the alterations in oxidative stress and ROS levels following exposure to MPs and NPs were assessed using the fluorochrome H₂DCFDA and confocal microscopy. For this, five daphnids were placed in 570 µL of ultrapure water and incubated with 30 µL of H₂DCFDA (1 mM in ultrapure water) for 30 min at 20 °C in the dark. Fluorescence images were acquired for each organism using a Leica TCS SP5 laser scanning confocal microscope. Additionally, biochemical analyses of LPO and total protein content were carried out on daphnids exposed to NPs. Twenty individuals were homogenized in 0.1 M ice-cold PBS (pH 7.2) and centrifuged at 10,000 rpm for 15 min at 4 °C [48]. The resulting supernatants (180 µL) were incubated with C4-BODIPY (20 µL, 50 µM in ultrapure water) for 30 min to assess LPO (excitation/emission 485/528 nm), and with a commercial QubitTM assay kit (20 µL QubitTM working solution, 30 min incubation, excitation/emission 485/590 nm) for total protein quantification. Fluorescence readings were taken using a Fluoroskan Ascent FL 96-well microplate reader.

3. Results

3.1. Particle charazterization

Table 1 presents the results for the characterization of all materials tested in this work in terms of concentration, ζ -potential and median particle size. UV irradiation of PPc and PPd led to the fragmentation of MPs, generating plastic particles with irregular shape within a wide size range. SEM micrographs of the MPs used in this study are presented in Figure S2, SM). Particle size measurements of UV-generated MPs confirmed the presence of particles in the 1-50 μm and 50-500 μm size ranges when dispersed in ultrapure water (Table 1). UV-254 nm irradiation produced MPs with larger particle sizes for PPc material compared to PPd material, likely due to the ability of IRG to act as hydroperoxide scavenger, thereby protecting the polymer backbone from degradation [29], [45]. Specifically, the statistical analysis of results showed significant difference (p < 0.05) between particles containing (PPc) and not containing (PPd) the additive (IRG). This result can be explained considering the additive is an antioxidant that prevents polymer degradation and, subsequent, particle fragmentation and in the absence of IRG the breakdown of the PP chain can progress further, leading to the formation of smaller particles. The addition of $\rm H_2O_2$ further reduced particle size; however, this effect was statistically significant (p < 0.05) only for PPc and its larger fraction (50-500 µm). This can be explained by the fact that the highly reactive, nonselective hydroxyl radicals generated by $\rm H_2O_2$ are less efficient at degrading IRG in larger particles. This process likely progressed rapidly, with no significant differences observed in the smaller particles, which had a higher external surface area exposed to oxidants [29], [31].

DLS measurements of NPs (< 1 µm) size showed the presence of particles in the few hundred nanometres range when dispersed in ultrapure water (Table 1). Comparing the particle size of the NPs generated upon irradiation, the influence of the antioxidant additive IRG in the plastic particles was not significant when irradiation took place with H₂O₂, which can be explained by the degradation and consumption of the antioxidant additive [29], [31]. However, the presence of additive, slightly suppressed fragmentation in the UV-irradiation without H₂O₂, with PPc particles breaking down to H_2O_2 from 383 ± 93 nm compared to 246 ± 21 nm for PPd. Full details of size distribution of all UV-generated NPs are provided in Figure S3 (SM). SEM micrographs (Figure S3) revealed that, in all cases, the surface of UV-generated MPs was rough, exhibiting holes and defects, indicating alterations in the polymer matrix. However, no significant morphological differences were observed between the UV-irradiation treatments, without or with H₂O₂, applied to the particles (Figure S3). All NP particles displayed negative charge as expected considering the hydrophobic character of PP particles and the asymmetry of the molecular charge distribution of hydroxide and hydronium ions, which makes the first more hydrophobic than the second and, therefore more prone to adsorb onto hydrophobic surfaces [20].

ATR-FTIR spectra of representative UV-generated plastic particles are presented in Figure S4 (SM). The spectra of the 50-500 μm MP fraction of both PPd and PPc material, predominantly displayed the bands characteristic of the PP polymer matrix. These include -CH₂ and -CH₃ stretching vibrations at 2850, 2920, and 2950 cm−1, as well as symmetric and asymmetric -CH₃ bending vibrations at 1376 and 1460 cm−1. Additionally, bands at 840, 1000, and 1165 cm−1 corresponding to typical vibrations of terminal unsaturated CH₂ groups in isotactic PP were identified. No detectable bands associated to IRG such as the C-O-P band at 1212 cm−1, or its potential UV-photodegradation by products were found on PPc material, likely due to the additive's low concentra-

tion within the polymeric matrix [16].

Figure S5 (SM) shows the chromatograms obtained from the analysis of the additives from the MPs particles of PPc non-irradiated, PPc irradiated without H_2O_2 , and PPc irradiated with H_2O_2 . The results reveal the presence of numerous compounds associated with PP oligomers containing varying numbers of repeating units, as well as the additive IRG. The primary difference between the virgin and irradiated materials is the greater consumption of IRG in the latter, leading to an increase in degradation-related species. For the sample irradiated in the presence of H₂O₂, a massive consumption of IRG and a significant reduction in oligomers, which may have migrated into the aqueous medium, are observed. To clarify this evolution in additive consumption, ions with m/z 191 and 206 were extracted from the chromatogram acquired in SCAN mode (Figure S5) and presented in Figure S6 (SM), as these ions are characteristic of fragments present in the degradation species and in the molecular structure of IRG. These findings corroborate the observations in Figure S5, which shows a higher ratio of degradation species to neat IRG, along with only residual levels of these compounds in the H₂O₂-treated sample.

3.2. Toxicity of microplastics

Irradiated MPs in the 1-50 μ m and 50-500 μ m size ranges, produced from the 100-500 μ m particles obtained through mechanical grinding of plastic pellets, were tested for toxicity using *D. magna* 48 h immobilization assays and *R. subcapitata* 72 h growth rate inhibition assays, as previously described. The SEM micrographs of MPs, in both size ranges and irradiated with and without H_2O_2 , are shown in Figure S2 confirming the presence of irregular particles in the specified ranges.

Fig. 1 (panels A1 to A4) shows the toxicity responses of *D. magna* to increasing concentrations of PPc and PPd-MPs or both size ranges, 1-50 µm and 50-500 µm produced either with UV irradiation in the presence and absence of H₂O₂. The results showed limited immobilization of daphnids due to either PPc-MPs or PPd-MPs. For the larger particle fractions (50-500 µm), the maximum immobilization effect was 27% and 20% for particles irradiated with and without H_2O_2 at 50 mg/L, respectively (A1 and A3). For the smaller particle fractions (1-50 µm), the maximum immobilization effect was 10% for MPs irradiated with H₂O₂ at 50 mg/L (A2 and A4). The effects observed for MPs in the 1–50 µm and 50–500 μm size ranges on *D. magna* can be attributed to physical damage. Supporting evidence includes particle aggregation and their attachment to the daphnids, which was more pronounced at higher MP concentrations, as shown in Figure S7. Potential effects due to ingestion are likely limited to particles smaller than 5 μ m, since 48h-old neonates can ingest particles up to that size, corresponding to the smaller fraction of MPs tested in this study [19]. There is also the possibility of a food dilution effect that could negatively affect daphnids; however, its impact is likely minimal, as discussed elsewhere [1].

Fig. 1 shows no significant toxicity differences on D. magna between PPc and PPd-MPs, despite differences in additive and non-polar oligomer content. GC-MS analyses (Figures S5 and S6) revealed that PPc contained the antioxidant additive IRG, its oxidized form tDtBPP, and the degradation product 2,4-DTBP. Upon the addition of H₂O₂ during irradiation, both IRG and tDtBPP were completely depleted from the plastic particles. The lack of significant toxicity differences between MPs irradiated with and without H₂O₂ suggests that the additive and its degradation products do not play a major role in the immobilization of *D. magna* neonates. This aligns with the fact that IRG and tDtBPP are expected to exhibit minimal migration from PPc-MPs into water under neutral pH conditions [13], [40]. Supporting this, IRG has a log K_{ow} (octanol-water partition coefficient) of 18.1 and a water solubility of only $5 \mu g/L$ at $20 \, ^{\circ}C$ (Source: ECHA Chemicals Database). Similarly, the log K_{ow} values for tDtBPP and 2,4-DTBP are also presumed to be high, estimated at 14.2 and 4.9, respectively, based on their chemical structures. Although 2,4-DTBP has shown moderate acute toxicity to D. magna, with an EC₅₀ of 0.5 mg/L (ECHA Chemicals Database), this concentration is well above the exposure levels reached in this study.

The effect on *R. subcapitata* after 72 h of exposure is also presented in Fig. 1 (panels B1 to B4). Contrary to the effect observed for *D. magna*, the results show considerable growth rate inhibition upon exposure to particles in the 1-50 µm range, particularly with PPc particles, and even more (90% inhibition) when the particles were irradiated with H_2O_2 . The fact that smaller particles led to higher toxicity can be explained by their greater surface area, which increases the potential for interaction with algal cells. Plastic particles, even when negatively charged, have been shown to interact with algal cells and inhibit growth, particularly in the case of aged microplastics compared to virgin ones [39]. The stronger effect of the more oxidized particles may be due to their increased surface roughness and higher degree of oxidation, which introduces functional groups that are more likely to interact with living cells [33]. Growth inhibition has been more frequently observed after short exposure periods and at intermediate particle concentrations [3]. Non-monotonic responses of algae to

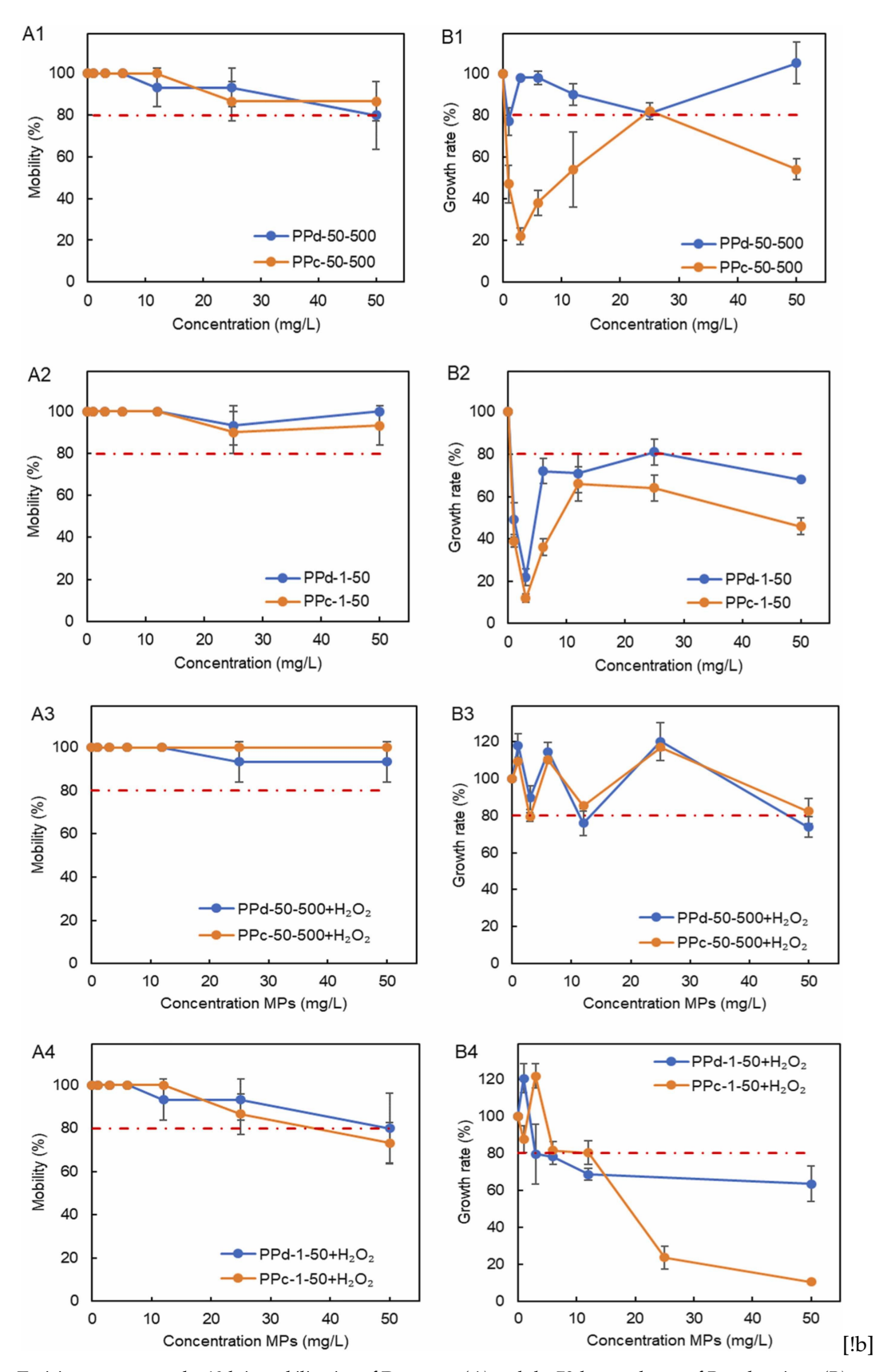


Figure 1: Toxicity response on the 48 h immobilization of D. magna (A) and the 72 h growth rate of R. subcapitata (B) upon exposure to PPc and PPd microplastic particles UV-generated with and without H_2O_2 . The dashed line represents EC_{20} (the concentration that causes 20% damage). Error bars represent the standard deviation. PPc: commercial PP containing IRG and PPO; PPd: additive-free PP; 50-500: microplastics within 50-500 μ m size range generated without H_2O_2 ; 1-50: microplastics within 1-50 μ m size range generated without H_2O_2 , 50-500+ H_2O_2 : MPs within 50-500 μ m size range generated with H_2O_2 , 1-50+ H_2O_2 : MPs within 1-50 μ m size range generated with H_2O_2 , 1-50+ H_2O_2 : MPs within 1-50 μ m size range generated with H_2O_2 , 1-50+ H_2O_2 : MPs within 1-50 μ m size range generated with H_2O_2 , 1-50+ H_2O_2 : MPs within 1-50 μ m size range generated with H_2O_2 . IRG: Irgafos-168 additive, PPO: PP oligomers.

increasing concentrations of MPs can be attributed to particle aggregation at high concentrations, which reduces the surface area available for cell interaction. This aggregation could reduce bioavailability and increase the turbidity of the exposure medium, as shown in Figure S8 (SM) [12].

The confocal micrographs shown in Figure S9, illustrate the observed toxicity behaviour of all UVgenerated MPs on algae cell density and Chl a autofluorescence. The smaller particle fraction (1-50 µm) reduced the Chl a pigment content of R. subcapitata compared to the larger particle fraction (50-500 µm), regardless of material type or photo-irradiation treatment, reflecting the growth status of cells and indicating inhibition of the algae's photosynthetic system in agreement with the results presented in Fig. 1 [4], [47]. It has been shown that PP with median particle size of 172 µm have been shown to reduce Chl a concentration in Chlorella pyrenoidosa and Microcystis flos-aquae, leading to a decline in the effective quantum yield of PSII and overall photosynthetic capacity [46]. It is also observed in Fig. 1 and S9 that PPc-MPs induced higher toxicity on algae than PPd-MPs, regardless of the photo-degradation conditions. This outcome could be attributed to the presence of IRG and its degradation products, tDtBPP and 2,4-DTBP (Figures S5 and S6), which may induce increased cell damage produced by the intrinsic properties of plastic particles [14], [26]. Non-polar compounds such as IRG and tDtBPP are expected to cause limited toxicity to algae in water, due to their low tendency to migrate from the bulk of the relatively large plastic particles. However, some chemical toxicity could arise from 2,4-DTBP, which has been reported to be hazardous for algae at an EC₅₀ of 0.37 mg/L (ECHA Chemicals Database).

3.3. Toxicity of nanoplastics

The NPs prepared in this work, whether from PPc or PPd, were tested for their toxicity for the 48 h immobilization of *D. magna* and the 72 h growth rate inhibition of *R. subcapitata*. The results are presented in Fig. 2 where the concentrations (expressed in mg/L) refer to the whole mass but essentially corresponded to the polymer (PP).

The results showed that the microcrustacean *D. magna* (Fig. 2A) was less affected than the algae *R. subcapitata* (Fig. 2B) by PPc and PPd NPs, similar to the trend observed with the MP fractions. However, the NPs generated from PPc and PPd exhibited higher toxicity in both organisms compared to MPs. The most toxic NPs for daphnids were PPc-NP+H₂O₂ and PPc-NP reaching 100% immobilization at 23 mg/L. The observed toxicity might be attributed to the combined inhibitory effect due to

the ingestion of NPs [19] and the presence of IRG and its related oxidation products, such as tDtBPP and 2,4-DTBP, which would be associated to the plastic particles rather than to the liquid fraction due to their low polarity [13-14, 26]. For the NPs generated from, PPc with H_2O_2 , PPc-NP+ H_2O_2 , enhanced toxicity may occur due to the presence of 2,4-DTBP, a photo-degradation product encountered in the plastic particles rather than in the liquid phase, again due to its low polarity (estimated log K_{ow} 4.9). These compounds would likely result in a 'Trojan horse' effect on *D. magna*, where nano-plastics originated from commercial plastics act as carriers for toxic compounds like the antioxidant IRG additive and its sub-products [37].

The NPs generated upon irradiation exhibited a high toxicity on algae, with the following growth rate inhibition effect: PPd-NP \approx PPd-NP+H2O2 > PPc-NP > PPc-NP+H2O2. At a concentration of 3 mg/L, NPs from PPc without and with H2O2 generated an inhibitory effect of 74% and 98%, respectively, while NPs from PPd resulted on 100% inhibitory effect. The higher toxicity of PPd NPs suggests that additives and their degradation products play a limited role, and that the interaction between particle aggregates and cells is the primary factor influencing toxicity. The higher aggregation of PPc was clearly observed in the confocal micrographs shown in Figure S13 (SM) and may explain their lower inhibitory effect compared to the NPs generated from PPd.

The role of the nano-plastics originating from PPc polymer as carriers for toxic hydrophobic compounds, namely residual PPO, and the antioxidant IRG additive (as well as its possible UV-degradation sub-products) was further investigated by comparing the effects of NPs from PPc with those of its constituents (PPO, IRG and EXT) together with PPd NPs (Fig. 3). The reason for using PPd NPs is that PPO, IRG and EXT are highly hydrophobic compounds that cannot be easily dispersed in water without the presence of a non-polar carrier.

The NPs generated from PPd, whether irradiated with or without H_2O_2 , exhibited the highest inhibitory effects on both D. magna and R. subcapitata when reloaded with EXT. This reloaded composition matched that of the original PPc. However, in this case, the oligomers and additives were just put in contact with the additive-free particles, making them more accessible than in the original PPc. It is noticeable that mixtures containing IRG become more toxic upon in oxidative irradiation (with the addition of H_2O_2 during photodegradation). This was likely due to a combined effect of NPs from PPd and the UV-degradation products of IRG, such as the identified tDtBPP and 2,4-DTBP. The NPs generated from PPc,

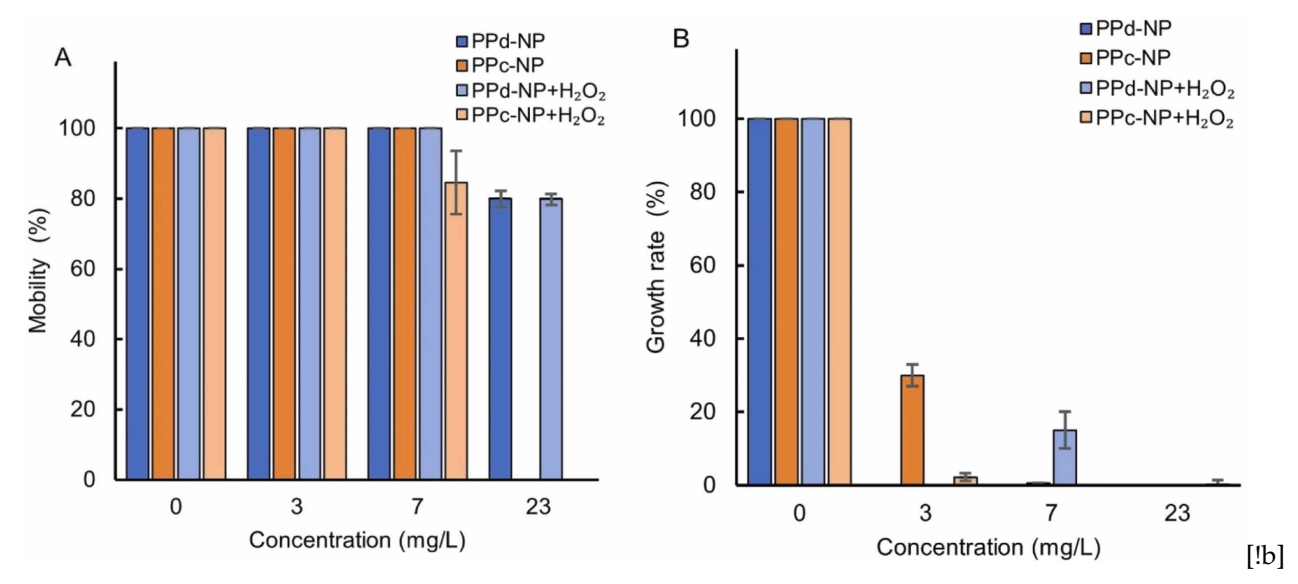


Figure 2: Effect of NPs generated from PPc and PPd for the 48 h immobilization of D. magna (A) and the 72 h growth rate inhibition of R. subcapitata (B). The error bars represent the standard deviation. PPc: commercial PP containing IRG and PPO, PPd: additive-free PP, NP: nanoplastics ($< 1 \mu m$) generated without H_2O_2 , NP+ H_2O_2 : nanoplastics ($< 1 \mu m$) generated with H_2O_2 .

consisting of particles which incorporated the additives from the original pellets were less toxic. This can be attributed to the lower availability of toxic compounds compared to the mixtures prepared in water. These results highlight the complex interactions between MPs, NPs, and chemicals, underscoring the need to consider multiple factors, such as particle size, photodegradation conditions, and organism type, when assessing the ecological impact of plastic debris in aquatic environments. The UVirradiated individual components, PPO, IRG, and EXT (containing PPO and IRG), both with and without H₂O₂, in the absence of plastic material, do not pose toxicity to algae and daphnids, which is explained by their poor solubility in water as they tend to migrate to the non-polar surfaces rather than remain bioavailable. The lack of significance (p > 0.05) of PPO, IRG, and EXT compared to controls is shown in Supporting Information as significance table displaying a pairwise comparison between two treatment groups for all materials, concentrations and for both organisms.

3.4. Toxicological endpoints

The main toxicological endpoints, EC₂₀ and LOEC, were calculated for *D. magna* (48 h immobilization) and *R. subcapitata* (72 h growth rate) following exposure to irradiated MPs and NPs from PPd and PPc particles, with and without H_2O_2 . The results are presented in Table 2. Generally, decreasing the size of plastic particles from 50 to 500 µm to 1-50 µm, and then to < 1 µm, resulted in higher immobilization of *D. magna*, with EC₂₀ values ranging from

 $58.0 \pm 1.2 \text{ mg/L}$ to $28.7 \pm 4.2 \text{ mg/L}$ for PPd and with EC₂₀ values ranging from > 50 mg/L to 7.2 \pm 0.1 mg/L for PPc (Table 2). Certainly, the plastic particles containing the IRG additive increased the negative effects on *D. magna*, suggesting that smaller particles are more easily ingested and cause greater harm by acting as carrier. Moreover, the addition of H₂O₂ in the irradiation treatment of PPc particles amplified their negative effects on D. magna, as a consequence of tDtBPP and 2,4-DTBP photo-degradation sub-products formation and their combined action. The EC₂₀ for NPs from PPc without H_2O_2 was 9.4 ± 4.2 mg/L, whereas with H_2O_2 , it decreased to 7.2 \pm 0.10 mg/L. In contrast, suspensions of NPs from PPd, which were free of additives, displayed lower toxicity, with EC₂₀ values of 28.7 ± 4.2 mg/L for particles UV-generated both without and with H_2O_2 .

The green alga R. subcapitata (72 h growth rate) was more sensitive to the MPs and NPs than the crustacean D. magna, with LOEC values of 1 and 3 mg/L (Table 2). Notably, the plastic particles containing the IRG additive UV-degraded with H₂O₂ increased the negative effects on R. subcapitata from an EC₂₀ value of 1.6 ± 0.4 mg/L for irradiated PPc without H_2O_2 , to an EC₂₀ of 0.2 ± 1.2 mg/L. In contrast, suspensions of PPd nanoparticles without additives displayed lower toxicity, with LOEC values of 3 mg/L for particles UV-generated both without and with H₂O₂. These suggested that, the interaction between plastic particles, IRG and its related photo-degradation sub-products, such as tDtBPP or 2,4-DTBP, likely resulted in an enhanced toxicity, increasing membrane cell damage and the overall toxicity of UV-generated PPc-MPs in algae.

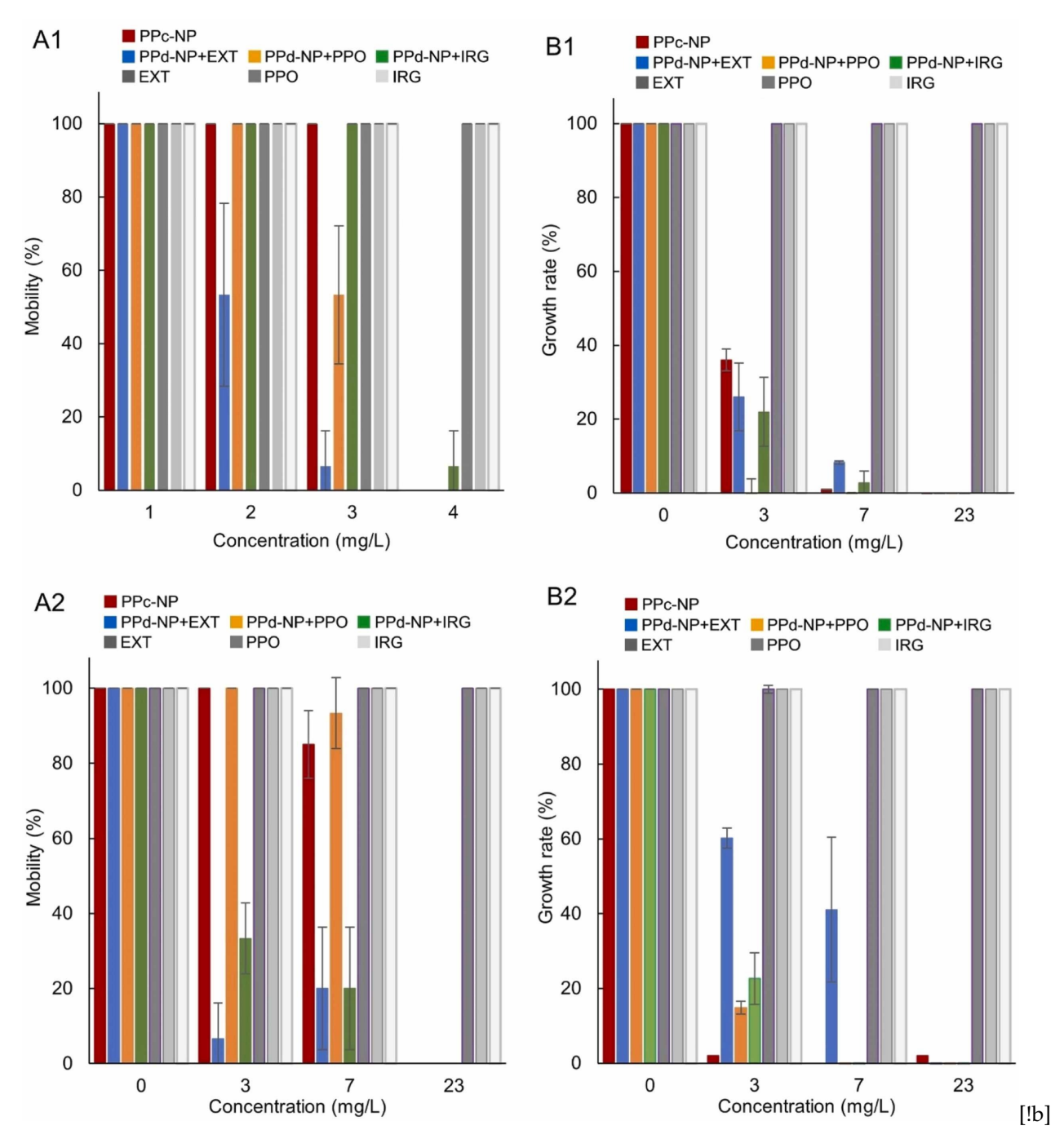


Figure 3: Effect of NPs from PPc (< 1 μ m) and re-additivated (after removing additives and oligomers) PPd, as well as the proportional amount of oligomers (PPO), additive (IRG), and extract (EXT, containing PPO and IRG) in irradiation runs with and without H_2O_2 for the 48 h immobilization of D. magna (A) and the 72 h growth rate inhibition of R. subcapitata (B), respectively: A1, B1 (without H_2O_2) and A2, B2 (with H_2O_2). The error bars represent the standard deviation. PPc: commercial PP containing IRG and PPO, PPd: additive-free PP; NP: NPs (< 1 μ m) generated without H_2O_2 ; NP+ H_2O_2 : NPs (< 1 μ m) generated with H_2O_2 .

Table 2. Main toxicological endpoints for the materials tested in this work.

Material	Sample	D. magna immobilization, 48 h	R. subcapitata growth rate, 72 h		
		EC ₂₀ (mg/L)	EC ₂₀ (mg/L)	LOEC (mg/L)	
	PPc-50-500	47.4 ± 0.8	-	1.0	
	PPc-50-500+H ₂ O ₂	>50	-	3.0	
DD -	PPc-1-50	50.6 ± 0.9	-	1.0	
PPc	PPc-1-50+H ₂ O ₂	41.4 ± 0.9	3.6 ± 0.4	-	
	PPc-NP	9.4 ± 4.2	1.6 ± 0.4	-	
	PPc-NP+H ₂ O ₂				
	PPd-50-500	46.2 ± 0.7	-	3.0	
	PPd-50-500+H ₂ O ₂	58.0 ± 1.2	-	3.0	
DD J	PPd-1-50	40.3 ± 0.9	-	1.0	
PPd	PPd-1-50+H ₂ O ₂	38.3 ± 0.7	12.3 ± 0.9	-	
	PPd-NP	28.7 ± 4.2	-	3.0	
	PPd-NP+H ₂ O ₂	23.0 ± 2.4	-	3.0	

EC₂₀: the concentration that causes 20% damage, LOEC: the lowest observed effect concentration, PPc: commercial PP containing IRG and PPO, PPd: additive-free PP, 50-500: MPs within 50-500 μm size range generated without H_2O_2 , 50-500+ H_2O_2 : MPs within 50-500 μm size range generated with H_2O_2 , 1-50: MPs within 1-50 μm size range generated without H_2O_2 , 1-50+ H_2O_2 : MPs within 1-50 μm size range UV-generated with H_2O_2 ; NP: NPs (< 1 μm) generated with H_2O_2 . The intervals (±) of EC20 represent 95% confidence intervals.

To get a further insight into this result, we performed an ANCOVA analysis. The results for R. subcapitata indicated that H₂O₂, particle size, and concentration had highly significant effects on the dependent variable (p < 0.001). The interaction concentration-size and H₂O₂-size were also significant (p < 0.001), which can be attributed to the higher specific surface offered for smaller particles. The presence of IRG is also significant (p < 0.05), while other interactions showed marginal significance. For D. magna the results are similar, indicating that concentration, size and the interaction H₂O₂-size were highly significant effects (p < 0.001). The other interactions with size were also significant (p < 0.01). This result can be explained considering the generally lower sizes of de-additivated plastics. Finally, the presence of IRG was significant at the p < 0.01 level. The detail of ANCOVA the results is shown as Supporting Information and show that, apart from the effect of concentration, plastic particle size was the main toxicity driver, with a considerable influence of the presence of the antioxidant additive (and its degradation products) in the exposure mixture and for both trophic levels.

3.5. Toxicity mechanisms

Intracellular ROS levels were quantified in *R. subcapitata* cells following exposure to MPs using H₂DCFDA. The results, shown in Figure S10 (Supplementary Material), panels A1 and A2, indicate a slight increase in ROS levels with larger

MPs (50-500 µm), but a substantial increase with smaller particles (1-50 µm), particularly with PPc at intermediate concentrations. Oxidative stress arises when there is an imbalance between ROS production and the antioxidant defence mechanisms giving rise to cellular damage [47]. This helps explain the results observed for membrane permeability, assessed using PI (panels B1 and B2), and esterase activity, measured using FDA (panels C1 and C2). Elevated ROS levels indicated that the algae were undergoing cellular stress, while combined FDA/PI staining revealed membrane damage in stressed cells, suggesting a transitional or partially compromised state. High ROS levels are frequently associated with oxidative damage to membrane lipids, which compromises membrane integrity and cell function, as well as with the disruption of photosynthesis and other metabolic pathways.

As previously discussed, the effects of MPs could be attributed to physical damage resulting from direct contact between plastic particles and algal cells. It has been shown that MPs can be physically adsorbed onto the surface of algal cells, and it is assumed that if they are small enough, they may act as a physical barrier to sunlight and oxygen, thereby stimulating ROS formation [49]. However, ROS overproduction has primarily been observed for NPs and only rarely and at high concentrations for MPs [25]. In our case, ROS generation was higher for the smaller particle fraction (1-50 µm) and for PPc MPs, which included the antioxidant in the same concentration as in the original pellets. This is also

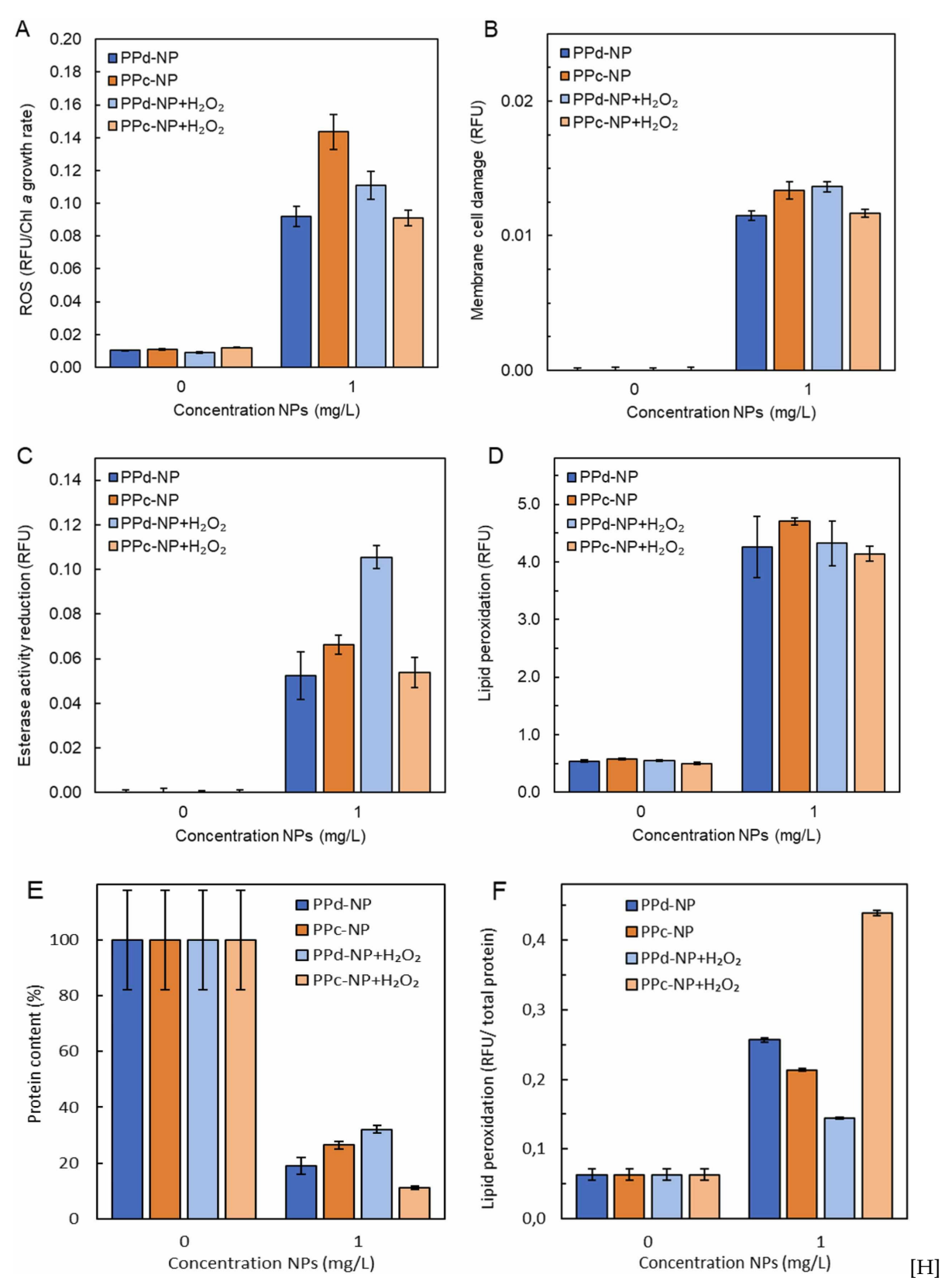


Figure 4: Alterations in key physiological parameters, after 72 h of exposure to 1 mg/L NPs generated in this study, of R. subcapitata: (A) ROS overproduction; (B) loss of membrane integrity; (C) reduction in esterase activity, and (D) LPO, as well as of D. magnaD. magna: (E) Total protein content and (F) LPO. Error bars represent the standard deviation. PPc: commercial PP containing IRG and PPO, PPd: additive-free PP.

observed in the confocal micrographs of Figure S11 (SM) that show the smaller particle fractions (1-50 µm) inducing greater ROS than the larger ones in *R. subcapitata*, as evidenced by the higher green fluorescence of the reaction of ROS with H₂DCFDA. The observed ROS imbalance and the associated membrane damage and metabolic alterations are better explained by exposure to the antioxidant additive IRG and its degradation products (tDtBPP and 2,4-DTBP), which aligns with the results shown in Fig. 1 and the confocal micrographs in Figure S8.

Concerning D. magna, Figure S12 (SM) shows confocal micrographs also revealing generalized oxidative stress after 48 h exposure to PPd and PPc MPs, 1-50 µm and 50-500 µm, generated with and without H_2O_2 . As observed in the images, control samples exhibited low fluorescent intensity, whereas the daphnids exposed to MPs displayed strong green fluorescence. In all cases, and regardless of particle size fraction, material, and irradiation treatment, the overproduction of ROS appeared to spread throughout the superficial layer of the D. magna body. These alterations might be related to physical impairment caused by direct contact rather than particle ingestion, as observed in Figure S7 using optical microscopy [22].

As explained in the preceding sections, the toxicity of NPs ($< 1 \mu m$), with EC₂₀ values in the mg/L range (PPc) was considerably higher than that of MPs, even for those in the lower size range of 1-50 μm. For the exposure of *R. subcapitata*, we also assessed changes in intracellular oxidative stress, lipid peroxidation, cell membrane integrity, and esterase activity in algal cells following exposure to the NPs used in this study. The results are presented in Fig. 4 (panels A to D) and demonstrate a clear increase in intracellular ROS following exposure to NPs. Notably, elevated ROS levels were observed at exposure concentrations below the EC₂₀ values, indicating sublethal effects. In parallel with increased ROS levels, R. subcapitata exhibited evident cell membrane damage and reduced esterase activity, suggesting that NPs may exert greater toxicity in aquatic environments. The effect of ROS causing LPO is also clear in Fig. 4 (panels A to D) and corresponds to the permeability changes and integrity of cell membranes.

The impact of small MPs and NPs on aquatic organisms has been shown to involve a cascade of effects triggered by the overproduction of ROS. Natarajan et al. reported increased oxidative stress and lipid peroxidation, along with decreased photosynthetic efficiency, membrane damage, and reduced esterase activity in the unicellular phytoplankton Scenedesmus obliquus exposed to 1 µm polystyrene particles [32]. Similar effects were observed in

Rhodomonas baltica following exposure to commercial poly(methyl methacrylate) NPs, including elevated ROS levels, lipid peroxidation, loss of membrane integrity, and reduced photosynthetic capacity [11]. Other studies have shown that oxidative stress induced by NPs in algal cells can damage membranes and intracellular structures, cause physical blockage, and impair photosynthetic activity in green algae [47, 5]. However, all of these studies used commercial nanoplastics. In contrast, our results are the first to use nanoplastics generated through a top-down approach, using fragmentation processes similar to those occurring in the environment.

The overproduction of ROS was also checked and found in D. magna after 48 h exposure to 1 mg/L of PPd and PPc NP that shows confocal micrographs corresponding to the fluorescence of H₂DCFDA. The control sample exhibited low fluorescent intensity, whereas the daphnids exposed to NPs showed strong fluorescence. Both PPd and PPc NPs, regardless of UV-irradiation treatment, resulted in strong fluorescent intensity throughout the D. magna body, indicating oxidative stress due to physical damage from direct external contact [41]. Notably, PPc NPs could be detected with strong fluorescent intensity in the hindgut of exposed daphnids (marked with an arrow in Figure S12). This indicates, not only internalization of NPs, but preferential oxidative stress in the digestive tract due to the ingestion of particles containing the remaining IRG additive and its degradation products, such as tDtBPP or 2,4-DTBP. In addition, *D. magna* exhibited a significant decrease in protein content (Fig. 4, panel E) and an increase in LPO levels (Fig. 4, panel F) following exposure to 1 mg/L of PPd and PPc NPs, indicating a disruption in lipid metabolism likely due to excessive ROS production in the organisms [30].

5. Conclusions

In this study, we assessed for the first time the aquatic toxicity of MPs (1-50 μ m and 50-500 μ m) and NPs (< 1 μ m) of commercial PP containing IRG as antioxidant additive (PPc) after exposure to conventional UV 254 nm germicidal radiation, both with and without H₂O₂, PP MPs and NPs without additive and oligomers (PPd) was also tested. Our findings revealed that the toxic effects were influenced by plastic particle size, concentration and the presence of additives. Smaller particles, the presence of IRG and its degradation products, and the oxidation produced by H₂O₂ contributed to higher toxicity in both the microcrustacean *D. magna* and the green alga *R. subcapitata*.

NPs from PPc (< 1 µm, containing IRG) exhibited

significant toxicity towards D. magna (48 h immobilization), with EC₂₀ values of and 7.2 ± 0.1 mg/L and 9.4 ± 4.2 mg/L for particles irradiated with and without H₂O₂, respectively. In contrast, suspensions of PPd NPs (< 1 µm) without additives displayed lower toxicity, with EC₂₀ of 28.7 ± 4.2 mg/L. The algae R. subcapitata (72 h growth rate) was more affected by NPs from PPc containing IRG than the crustacean D. magna, with EC₂₀ values of 0.2 ± 1.2 mg/L and 1.6 ± 0.4 mg/L for particles irradiated with and without H₂O₂, respectively. In contrast, suspensions of PPd nanoparticles without additives displayed lower toxicity, with LOEC values of 3 mg/L.

These results showed that particles from commercial plastics can act as carriers for toxic non-polar compounds, such as the antioxidant additive IRG and its transformation products, thereby amplifying negative effects on the aquatic organisms D. magna and R. subcapitata. The toxicity observed in R. subcapitata was accompanied by increased production of intracellular ROS, LPO, loss of membrane integrity, and impairment of esterase activity. In D. magna, toxicity was driven by the generation of ROS, with effects detected in the hindgut following NP ingestion. Our study highlights the multidimensional effects of plastic particles under photodegradation scenarios, emphasizing the role of micro- and nanoparticles from commercial plastics containing additives and their toxicological implications for aquatic biota.

Acknowledgements

The authors acknowledge the financial support provided by the Spanish Government, Ministry of Science, grants PID2020–113769RB-C21/C22, PID2020–114930GB-I00, PLEC2021–007693 and TED2021–131609B-C32/33. GA thanks to the Spanish Government, Ministry of Science, Innovation and Universities, for her 'Beatriz Galindo' BG22/00043 grant and Community of Madrid, grant CM/BG/2023–001..

References

- [1] G. Amariei, R. Rosal, F. Fernández-Piñas, A.A. Koelmans. Negative food dilution and positive biofilm carrier effects of microplastic ingestion by *D. magna* cause tipping points at the population level. Environ Pollut, 294 (2022), 118622, 10.1016/j.envpol.2021.118622.
- [2] A.L. Andrady, P.W. Barnes, J.F. Bornman, T. Gouin, S. Madronich, C.C. White, R.G. Zepp, M.A.K. Jansen. Oxidation and fragmentation of plastics in a changing environment; from UV-radiation to biological degradation. Sci Total Environ, 851 (2022), 158022,

- 10.1016/j.scitotenv.2022.158022.
- [3] M. Baudrimont, A. Arini, C. Guégan, Z. Venel, J. Gigault, B. Pedrono, J. Prunier, L. Maurice, A. Ter Halle, A. Feurtet-Mazel. Ecotoxicity of polyethylene nanoplastics from the North Atlantic oceanic gyre on freshwater and marine organisms (microalgae and filter-feeding bivalves). Environ Sci Pollut Res, 27 (4) (2020), 3746-3755, 10.1007/s11356-019-04668-3.
- [4] E. Besseling, B. Wang, M. Lürling, A.A. Koelmans. Nanoplastic affects growth of *S. obliquus* and reproduction of *D. magna*. Environ Sci Technol, 48 (20) (2014), 12336-12343, 10.1021/es503001d.
- [5] P. Bhattacharya, S. Lin, J.P. Turner, P.C. Ke. Physical adsorption of charged plastic nanoparticles affects algal photosynthesis. J Phys Chem C, 114 (39) (2010), 16556-16561, 10.1021/jp1054759.
- [6] E. Blázquez-Blázquez, J. Lahoz, E. Pérez, M.L. Cerrada. An effective package of antioxidants for avoiding premature failure in polypropylene random copolymer plastic pipes under hydrostatic pressure and high temperature. Polymers, 13 (16) (2021), 10.3390/polym13162825.
- [7] D.G. Bucknall. Plastics as a materials system in a circular economy. Philos Trans R Soc A: Math, Phys Eng Sci, 378 (2176) (2020), p. 20190268, 10.1098/rsta.2019.0268.
- [8] T.-C. Chou. Theoretical basis, experimental design, and computerized simulation of synergism and antagonism in drug combination studies Pharmacol Rev, 58 (3) (2006), 621-681, 10.1124/pr.58.3.10.
- [9] V. Fauvelle, M. Garel, C. Tamburini, D. Nerini, J. Castro-Jiménez, N. Schmidt, A. Paluselli, A. Fahs, L. Papillon, A.M. Booth, R. Sempéré. Organic additive release from plastic to seawater is lower under deep-sea conditions. Nat Commun, 12 (1) (2021), 4426, 10.1038/s41467-021-24738-w.
- [10] J. Gigault, H. El Hadri, B. Nguyen, B. Grassl, L. Rowenczyk, N. Tufenkji, S. Feng, M. Wiesner. Nanoplastics are neither microplastics nor engineered nanoparticles. Nat Nanotechnol, 16 (5) (2021), 501-507, 10.1038/s41565-021-00886-4.
- [11] T. Gomes, A.C. Almeida, A. Georgant-zopoulou. Characterization of cell responses in Rhodomonas baltica exposed to PMMA nanoplastics Sci Total Environ, 726 (2020), 138547, 10.1016/j.scitotenv.2020.138547.
- [12] S. Gonzalo, V. Llaneza, G. Pulido-Reyes, F. Fernández-Piñas, J.C. Bonzongo, F. Leganes, R. Rosal, E. García-Calvo, I. Rodea-Palomares. A colloidal singularity reveals the crucial role of colloidal stability for nanomaterials In-vitro toxicity testing: nZVI-nicroalgae colloidal system

- as a case study PLoS One, 9 (10) (2014), e109645, 10.1371/journal.pone.0109645.
- [13] N. Haider, S. Karlsson. Kinetics of migration of antioxidants from polyolefins in natural environments as a basis for bioconversion studies Biomacromolecules, 1 (2000), 7, 10.1021/bm0000283.
- [14] C. Han, J. Ren, B. Wang, Z. Wang, H.B. Yin, F. Ke, D. Xu, L. Zhang, X. Si, Q. Shen. Ignored effects of phosphite (P(+III)) on the growth responses of three typical algae species Environ Pollut, 294 (2022), 118672, 10.1016/j.envpol.2021.118672.
- [15] L. Hermabessiere, J. Receveur, C. Himber, D. Mazurais, A. Huvet, F. Lagarde, C. Lambert, I. Paul-Pont, A. Dehaut, R. Jezequel, P. Soudant, G. Duflos. An Irgafos® 168 story: When the ubiquity of an additive prevents studying its leaching from plastics. Sci Total Environ, 749 (2020), 141651, 10.1016/j.scitotenv.2020.141651.
- [16] J. Hernández-Fernández, H. Cano, A.F. Reyes. Valoration of the synthetic antioxidant tris-(diterbutyl-phenol)-phosphite (Irgafos P-168) from industrial wastewater and application in polypropylene matrices to minimize its thermal degradation. Molecules, 28 (7) (2023), 3163, 10.3390/molecules28073163.
- [17] ISO. Water quality Determination of the Inhibition of the Mobility of *Daphnia magna* Straus (Cladocera, Crustacea) Acute Toxicity Test. ISO 6341:2012. International Organization for Standardization, Geneva (2012).
- [18] ISO. Water quality Fresh Water Algal Growth Inhibition Test with Unicellular Green Algae. ISO I8692:2012. International Organization for Standardization, Geneva (2012).
- [19] E. Kelpsiene, O. Torstensson, M.T. Ekvall, L.A. Hansson, T. Cedervall. Long-term exposure to nanoplastics reduces life-time in *Daphnia magna*. Sci Rep, 10 (1) (2020), 5979, 10.1038/s41598-020-63028-1.
- [20] K.N. Kudin, R. Car. Why are water-hydrophobic interfaces charged? J Am Chem Soc, 130 (12) (2008), 5.
- [21] W. Liu, S.A. Andrews, M.I. Stefan, J.R. Bolton. Optimal methods for quenching $\rm H_2O_2$ residuals prior to UFC testing. Water Res, 37 (15) (2003), 3697-3703, 10.1016/S0043-1354(03)00264-1.
- [22] A. Luangrath, J. Na, P. Kalimuthu, J. Song, C. Kim, J. Jung. Ecotoxicity of polylactic acid microplastic fragments to *Daphnia magna* and the effect of ultraviolet weathering. Ecotox Environ Saf, 271 (2024), 115974, 10.1016/j.ecoenv.2024.115974.
- [23] N.R. Maddela, D. Kakarla, K. Venkateswarlu, M. Megharaj. Additives of plastics: entry into the

- environment and potential risks to human and ecological health. J Environ Manag, 348 (2023), 119364, 10.1016/j.jenvman.2023.119364.
- [24] A.A. Mamun, T.A.E. Prasetya, I.R. Dewi, M. Ahmad. Microplastics in human food chains: Food becoming a threat to health safety. Sci Total Environ, 858 (2023), 159834, 10.1016/j.scitotenv.2022.159834.
- [25] Y. Mao, H. Ai, Y. Chen, Z. Zhang, P. Zeng, L. Kang, W. Li, W. Gu, Q. He, H. Li. Phytoplankton response to polystyrene microplastics: Perspective from an entire growth period. Chemosphere, 208 (2018), 59-68, 10.1016/j.chemosphere.2018.05.170.
- [26] G.M. Marielle, C. Durrieu, A. Guenne, L. Rouillac, D. Diafi, I. Nour, L. Mazéas, T.F. Nathalie, F. Farcas. Impact of polyethylene and polypropylene geomembranes in sensitive aquatic environment. Ecotoxicol Environ Saf, 148 (2018), 884-891, 10.1016/j.ecoenv.2017.11.015.
- [27] L. Maringer, L. Roiser, G. Wallner, D. Nitsche, W. Buchberger. The role of quinoid derivatives in the UV-initiated synergistic interaction mechanism of HALS and phenolic antioxidants. Polym Degrad Stab, 131 (2016), 91-97, 10.1016/j.polymdegradstab.2016.07.007.
- [28] L.C. Markley, A.M. González Bonet, A. Ogungbesan, O.J. Bandele, A.B. Bailey, G.W. Patton. Safety assessment for tris(2,4-di-tert-butylphenyl) phosphite (Irgafos 168) used as an antioxidant and stabilizer in food contact applications. Food Chem Toxicol, 178 (2023), 113877, 10.1016/j.fct.2023.113877.
- [29] N. Meides, A. Mauel, T. Menzel, V. Altstädt, H. Ruckdäschel, J. Senker, P. Strohriegl. Quantifying the fragmentation of polypropylene upon exposure to accelerated weathering. Micro Nanoplastics, 2 (1) (2022), 10.1186/s43591-022-00042-2.
- [30] S.S. Nagaraja, Y. Gouda, D. Miguez, Y. Muralidaran, L.F. Romanholo Ferreira, J.H.P. Américo-Pinheiro, S.I. Mulla, P. Mishra. Distinctive toxic repercussions of polystyrene nano plastic towards aquatic non target species Nitrobacter vulgaris, Scenedesmus sp. and *Daphnia magna*. Ecotoxicology, 34 (1) (2025), 61-75, 10.1007/s10646-024-02810-7.
- [31] H. Nakatani, Y. Ohshima, T. Uchiyama, S. Motokucho. Degradation and fragmentation behavior of polypropylene and polystyrene in water. Sci Rep, 12 (1) (2022), 18501, 10.1038/s41598-022-23435-y.
- [32] L. Natarajan, D. Soupam, S. Dey, N. Chandrasekaran, R. Kundu, S. Paul, A. Mukherjee. Toxicity of polystyrene microplastics in fresh-

- water algae Scenedesmus obliquus: effects of particle size and surface charge. Toxicol Rep, 9 (2022), 1953-1961, 10.1016/j.toxrep.2022.10.013.
- [33] T.M. Nolte, N.B. Hartmann, J.M. Kleijn, J. Garnæs, D. van de Meent, A. Jan Hendriks, A. Baun. The toxicity of plastic nanoparticles to green algae as influenced by surface modification, medium hardness and cellular adsorption. Aquat Toxicol, 183 (2017), 11-20, 10.1016/j.aquatox.2016.12.005.
- [34] OECD. CAS No. 31570-04-4- SIDS Initial Assessment Profile, SIAM 18, 20-23 April. Paris (2004).
- [35]OECD. Test No. 202: Daphnia sp. Acute Immobilisation Test. Guidelines for the Testing of Chemicals, Section 2. Organisation for Economic Cooperation and Development, Paris (2004).
- [36] R Core Team. R: A Language and Environment for Statistical Computing. Vienna (2022).
- [37] M.E. Schiano, C. Edo, E. Blázquez-Blázquez, M.L. Cerrada, F. Fernández-Pinas, R. Rosal. Use of a nanoplastic carrier for assessing the aquatic toxicity of an organo-phosphite polymer additive. Environ Pollut, 361 (2024), 124837, 10.1016/j.envpol.2024.124837.
- [38] J.M. Sipe, N. Bossa, W. Berger, N. von Windheim, K. Gall, M.R. Wiesner. From bottle to microplastics: can we estimate how our plastic products are breaking down? Sci Total Environ, 814 (2022), 152460, 10.1016/j.scitotenv.2021.152460.
- [39] W. Song, C. Fu, Y. Fang, Z. Wang, J. Li, X. Zhang, K. Bhatt, L. Liu, N. Wang, F. Liu, S. Zhu. Single and combined toxicity assessment of primary or UV-aged microplastics and adsorbed organic pollutants on microalga *Chlorella pyrenoidosa*. Environ Pollut, 318 (2023), 120925, 10.1016/j.envpol.2022.120925.
- [40] S. Sridharan, M. Kumar, M. Saha, M.B. Kirkham, L. Singh, N.S. Bolan. The polymers and their additives in particulate plastics: What makes them hazardous to the fauna? Sci Total Environ, 824 (2022), 153828, 10.1016/j.scitotenv.2022.153828.
- [41] M. Tamayo-Belda, A.V. Pérez-Olivares, G. Pulido-Reyes, K. Martin-Betancor, M. González-Pleiter, F. Leganés, D.M. Mitrano, R. Rosal, F. Fernández-Piñas. Tracking nanoplastics in freshwater microcosms and their impacts to aquatic organisms. J Hazard Mater, 445 (2023), 130625, 10.1016/j.jhazmat.2022.130625.
- [42] Y.-H. Tsai, P.J. Lein. Mechanisms of organophosphate neurotoxicity. Curr Opin Toxicol, 26 (2021), 49-60, 10.1016/j.cotox.2021.04.002.
- [43] UNEP. Chemicals in plastics: A technical report, in: United Nations Environment Programme, S.o.t.B., Rotterdam and Stockholm Conventions

- (Ed.). Geneva (2023).
- [44] Z. Wang, G. Liang, S. Jiang, F. Wang, H. Li, B. Li, H. Zhu, A. Lu, W. Gong. Understanding the environmental impact and risks of organic additives in plastics: A call for sustained research and sustainable solutions. Emerg Contam, 10 (4) (2024), 100388, 10.1016/j.emcon.2024.100388.
- [45] X. Wu, P. Liu, H. Shi, H. Wang, H. Huang, Y. Shi, S. Gao .Photo aging and fragmentation of polypropylene food packaging materials in artificial seawater. Water Res, 188 (2021), 116456, 10.1016/j.watres.2020.116456.
- [46] Y. Wu, P. Guo, X. Zhang, Y. Zhang, S. Xie, J. Deng. Effect of microplastics exposure on the photosynthesis system of freshwater algae J Hazard Mater, 374 (2019), 219-227, 10.1016/j.jhazmat.2019.04.039.
- [47] Z. Yan, L. Xu, W. Zhang, G. Yang, Z. Zhao, Y. Wang, X. Li. Comparative toxic effects of microplastics and nanoplastics on Chlamydomonas reinhardtii: Growth inhibition, oxidative stress, and cell morphology. J Water Process Eng, 43 (2021), 102291, 10.1016/j.jwpe.2021.102291.
- [48] D. Yuan, B. Zhang. Assessing the chronic toxicity of climbazole to *Daphnia magna*: Physiological, biochemical, molecular, and reproductive perspectives. Comp Biochem Physiol C: Toxicol Pharm, 287 (2025), 110061, 10.1016/j.cbpc.2024.110061.
- [49] Z. Zhao, X. Zheng, Z. Han, S. Yang, H. Zhang, T. Lin, C. Zhou. Response mechanisms of Chlorella sorokiniana to microplastics and PFOA stress: photosynthesis, oxidative stress, extracellular polymeric substances and antioxidant system. Chemosphere, 323 (2023), 138256, 10.1016/j.chemosphere.2023.138256.

Supplementary Materials

Aquatic toxicity of UV-irradiated commercial polypropylene plastic particles and associated chemicals

Laura Contreras-Castillo¹, Enrique Blázquez-Blázquez², María L. Cerrada², Georgiana Amariei^{1,*}, Roberto Rosal¹

Contents:

- **Figure S1**. Emission spectrum of the 15 W Heraeus Noblelight TNN 15/32 low pressure mercury vapour lamp (UV) emitting at 254 nm, used for irradiation experiments.
- **Figure S2**. Scanning electron microscopy micrographs of the microplastics used in this study.
- **Figure S3**. Size distribution of UV-generated NPs measured by DLS. A-I: additive-free PP NPs irradiated without H_2O_2 , PPd-NP; A-II: additive-free PP NPs irradiated with H_2O_2 , PPd-NP+ H_2O_2 ; B-I: NPs generated from commercial PP containing 0.037 wt% IRG and 0.2 wt% oligomers without H_2O_2 , PPc-NP); B-II: NPs generated from commercial PP containing 0.037 wt% IRG and 0.2 wt % oligomers with H_2O_2 , PPc-NP+ H_2O_2).
- **Figure S4**. ATR-FTIR spectra of the 50-500 μ m MPs generated in this work. PPc: commercial PP containing IRG and PPO, PPd: additive-free PP, 50-500: MPs within 50-500 μ m size range generated without H₂O₂, 50-500+H₂O₂: MPs within 50-500 μ m size range generated with H₂O₂. IRG: Irgafos-168 additive, PPO: PP oligomers.
- **Figure S5**. GC-MS cchromatograms obtained from PPc plastic particles: non-irradiated, irradiated for 10 min without H_2O_2 (PPc-1-500), and irradiated for 10 min with H_2O_2 (PPc-1-500+ H_2O_2). The numbers indicate IRG and its degradation products. 1: 2,4-Di-tert-butylphenol (CAS# 96-76-4), 2: Irgafos 168 (IRG, CAS# 31570-04-4), and 3: oxidized form of IRG (CAS# 95906-11-9).
- **Figure S6**. Ions with m/z 191 and 206 extracted from chromatograms acquired in SCAN mode in Figure S5. The numbers indicate IRG and its degradation products. 1: 2,4-di-tert-butylphenol (CAS# 96-76-4), 2: Irgafos 168 (IRG, CAS# 31570-04-4), and 3: oxidized form of IRG (CAS# 95906-11-9). The asterisk indicates other structures related to IRG.
- **Figure S7**. Optical micrographs corresponding to *D. magna* immobilization upon 48 h exposure to the MPs tested in this work (50-500 μm and 1-50 μm). PPc: commercial PP containing IRG and PPO, PPd: additive-free PP, 50-500: MPs within 50-500 μm size range

¹Department of Chemical Engineering, Universidad de Alcalá, E-28871 Alcalá de Henares, Madrid, Spain ²Instituto de Ciencia y Tecnología de Polímeros (ICTP-CSIC), Juan de la Cierva 3, Madrid 28006, Spain

^{*} Corresponding author: georgiana.amariei@uah.es

generated without H_2O_2 , $50-500+H_2O_2$: MPs within $50-500~\mu m$ size range generated with H_2O_2 , 1-50: MPs within $1-50~\mu m$ size range generated without H_2O_2 , $1-50+H_2O_2$: MPs within $1-50~\mu m$ size range generated with H_2O_2 . IRG: Irgafos-168 additive, PPO: PP oligomers.

Figure S8. Turbidity of all tested suspensions of MPs irradiated without H_2O_2 (A-I: 50-500 μm; A-II: 1-50 μm) and with H_2O_2 (B-I: 50-500 μm; B-II: 1-50 μm), in *R. subcapitata* algae growth medium after 72 h of abiotic incubation. Error bars represent standard deviation. PPc: commercial PP containing IRG and PPO, PPd: additive-free PP, 50-500: MPs within 50-500 μm size range generated without H_2O_2 , 50-500+ H_2O_2 : MPs within 50-500 μm size range generated with H_2O_2 , 1-50: MPs within 1-50 μm size range generated without H_2O_2 , 1-50+ H_2O_2 : MPs within 1-50 μm size range generated with H_2O_2 . IRG: Irgafos-168 additive, PPO: PP oligomers.

Figure S9. Confocal micrographs (Bright-Field and Chl *a* ($\lambda_{ex.}$ 488 nm, $\lambda_{em.}$ 595-700 nm) corresponding to growth rate of *R. subcapitata* upon 72 h exposure to a concentration of 3 mg/L of all MPs tested in this work. PPc: commercial PP containing IRG and PPO, PPd: additive-free PP, 50-500: MPs within 50-500 μm size range generated without H₂O₂, 50-500+H₂O₂: MPs within 50-500 μm size range generated with H₂O₂, 1-50: MPs within 1-50 μm size range generated with H₂O₂. IRG: Irgafos-168 additive, PPO: PP oligomers.

Figure S10. Alterations on relevant parameters of *R. subcapitata* after 72 h of exposure to all MPs generated in this work: (A) generalized oxidative stress; (B) membrane integrity; (C) metabolic- esterase activity. A1, B1, C1 (50-500 μm) and A2, B2, C2 (1-50 μm). Results are shown as RFU normalized with respect to the percentage of algal growth. Error bars represent the standard deviation. PPc: commercial PP containing IRG and PPO, PPd: additive-free PP, 50-500: MPs within 50-500 μm size range generated without H_2O_2 , H_2O_2 : MPs within 50-500 μm size range generated with H_2O_2 , H_2O_2 : MPs within 1-50 μm size range generated with H_2O_2 , H_2O_2 : MPs within 1-50 μm size range generated with H_2O_2 . IRG: Irgafos-168 additive, PPO: PP oligomers.

Figure S11. Confocal micrographs corresponding to generalized oxidative stress, ROS, produced on *R. subcapitata* upon 72 h exposure to a concentration of 1 mg/L of all MPs and NPs tested in this work. PPc: commercial PP containing IRG and PPO, PPd: additive-free PP, 50-500: MPs within 50-500 μm size range generated without H_2O_2 , 50-500+ H_2O_2 : MPs within 50-500 μm size range generated with H_2O_2 , 1-50: MPs within 1-50 μm size range generated with H_2O_2 , NP: NPs (< 1 μm) generated with H_2O_2 , NP+ H_2O_2 : NPs (< 1 μm) generated with H_2O_2 . IRG: Irgafos-168 additive, PPO: PP oligomers.

Figure S12. Confocal micrographs corresponding to generalized oxidative stress, ROS, status on D. magna upon 72 h exposure to a concentration of 50 mg/L of PPd and PPc MPs (within 1-50 µm and 50-500 µm size ranges) and 1 mg/L PPd and PPc NPs UV-generated, without and with H_2O_2 , respectively. PPc: commercial PP containing IRG and PPO, PPd: additive-free polypropylene. IRG: Irgafos-168 additive, PPO: PP oligomers.

Figure S13. Confocal micrographs (Bright-Field and Chl *a* ($\lambda_{ex.}$ 488 nm, $\lambda_{em.}$ 595-700 nm) corresponding to growth rate of *R. subcapitata* upon 72 h exposure to 3 mg/l of all NPs tested in this work. PPc: commercial PP containing IRG and PPO, PPd: additive-free PP; NP: NPs (< 1 µm) generated without H₂O₂, NP+H₂O₂: NPs (< 1 µm) generated with H₂O₂.

IRG: Irgafos-168 additive, PPO: PP oligomers.

Analyses of statistical significance. Pairwise comparison between treatments. Shadowed cells represent significant differences (p < 0.05).

ANCOVA statistical analyses. For R. subcapitata (A) and D. magna (B). IRG and H_2O_2 are categorical variables. Size (taken from Table 1) and concentrations are continuous variables.

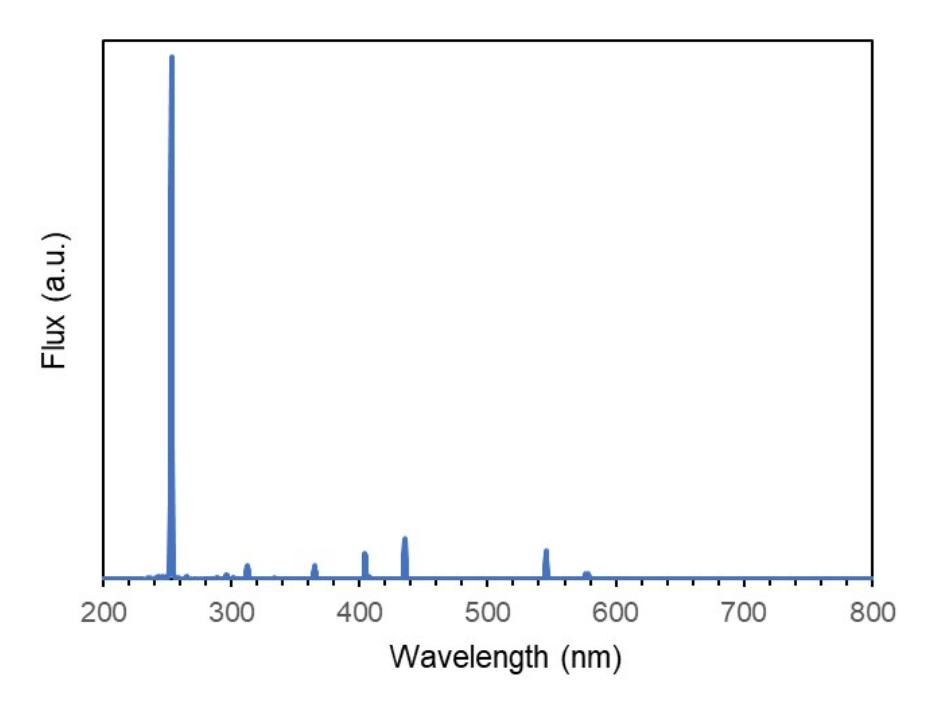


Figure S1: Emission spectrum of the 15 W Heraeus Noblelight TNN 15/32 low pressure mercury vapour lamp (UV) emitting at 254 nm, used for irradiation experiments.

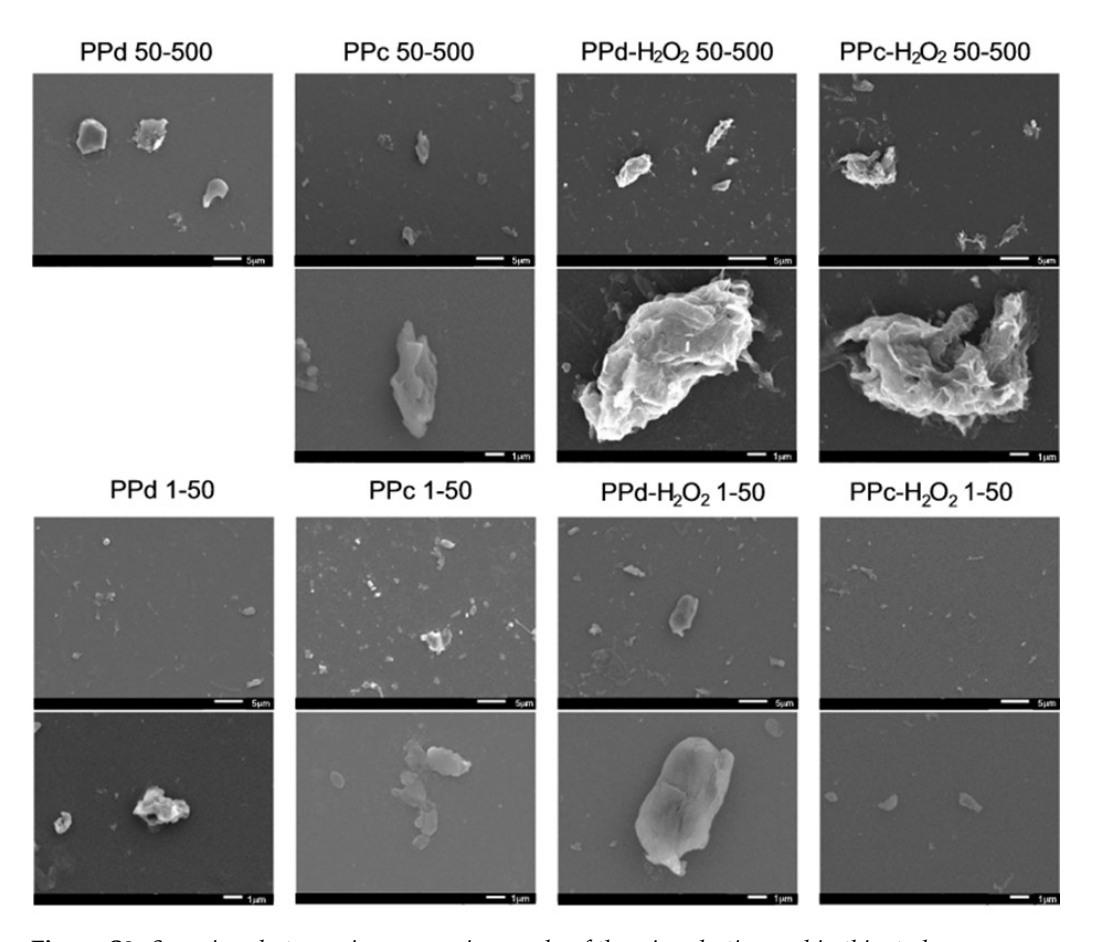


Figure S2: Scanning electron microscopy micrographs of the microplastics used in this study.

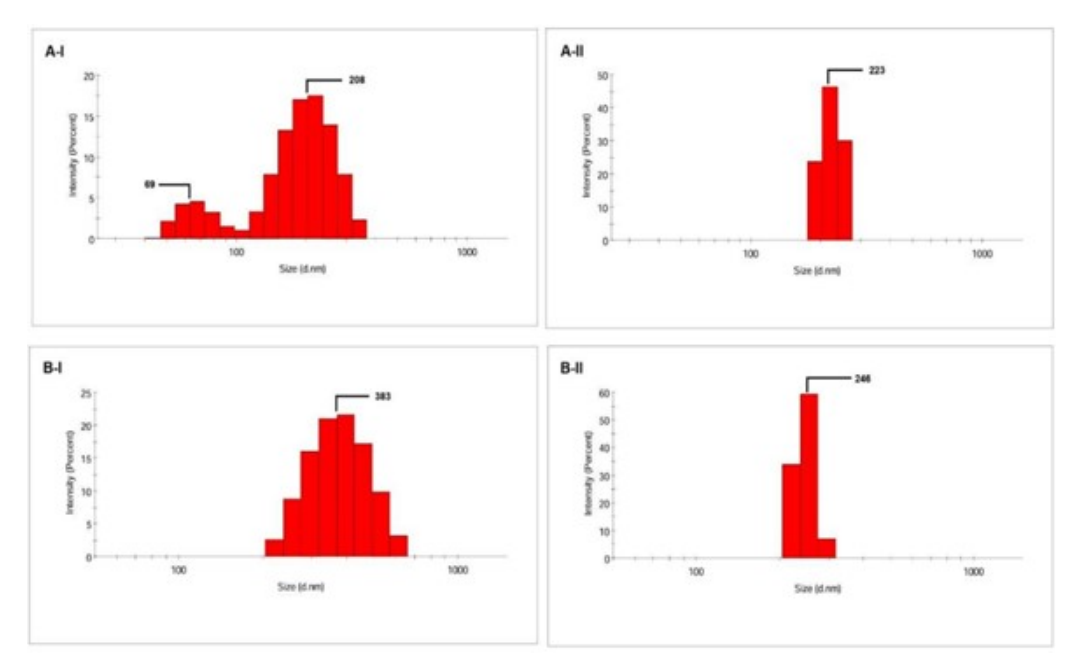


Figure S3: Size distribution of UV-generated NPs measured by DLS. A-I: additive-free PP NPs irradiated without H_2O_2 , PPd-NP; A-II: additive-free PP NPs irradiated with H_2O_2 , PPd-NP+ H_2O_2 ; B-I: NPs generated from commercial PP containing 0.037 wt% IRG and 0.2 wt% oligomers without H_2O_2 , PPc-NP); B-II: NPs generated from commercial PP containing 0.037 wt% IRG and 0.2 wt% oligomers with H_2O_2 , PPc-NP+ H_2O_2).

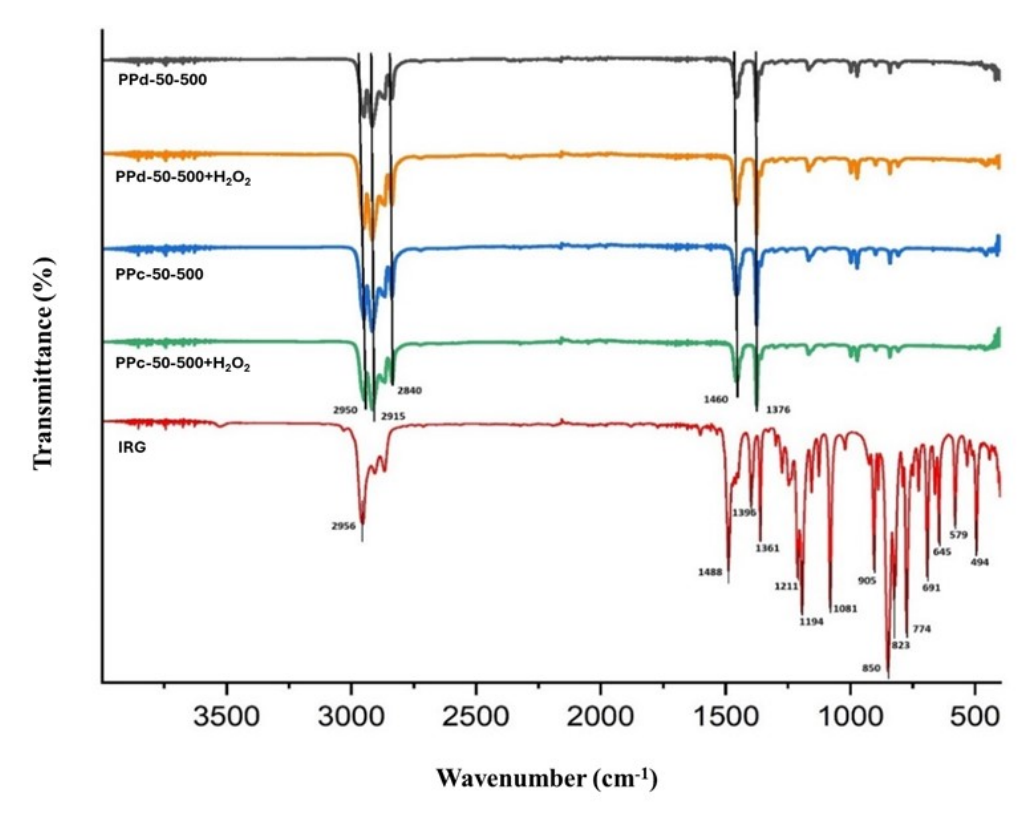


Figure S4: ATR-FTIR spectra of the 50-500 μ m MPs generated in this work. PPc: commercial PP containing IRG and PPO, PPd: additive-free PP, 50-500: MPs within 50-500 μ m size range generated without H_2O_2 , 50-500+ H_2O_2 : MPs within 50-500 μ m size range generated with H_2O_2 . IRG: Irgafos-168 additive, PPO: PP oligomers.

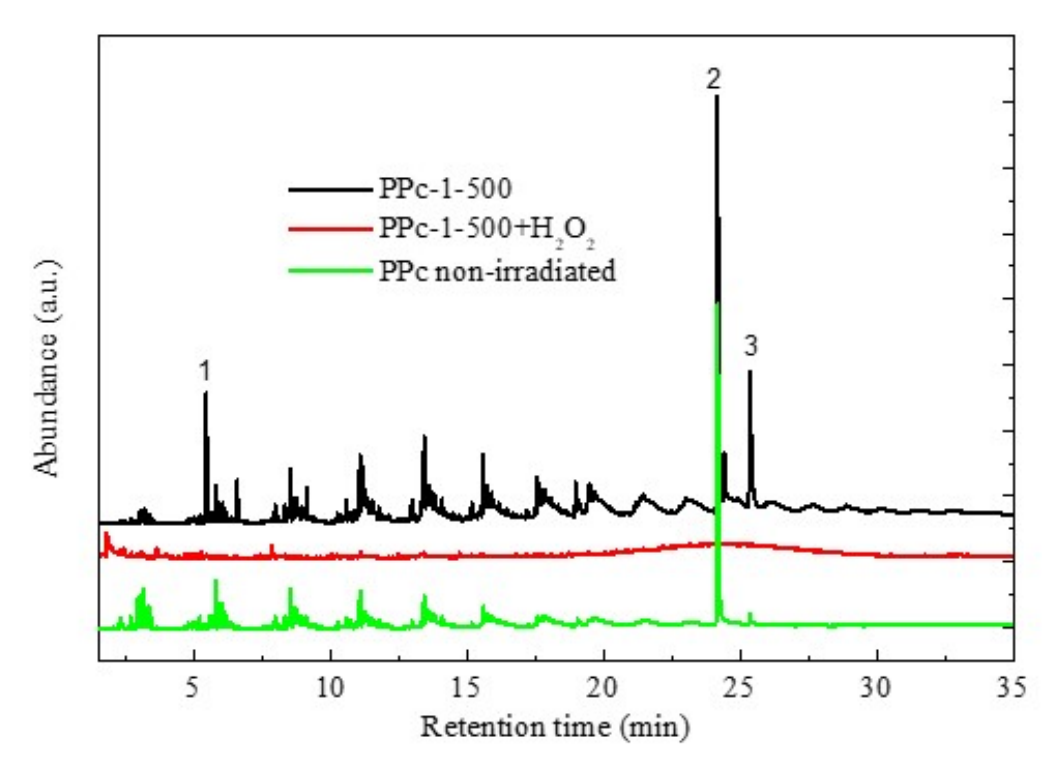


Figure S5: GC-MS cchromatograms obtained from PPc plastic particles: non-irradiated, irradiated for 10 min without H_2O_2 (PPc-1-500), and irradiated for 10 min with H_2O_2 (PPc-1-500+ H_2O_2). The numbers indicate IRG and its degradation products. 1: 2,4-Di-tert-butylphenol (CAS# 96-76-4), 2: Irgafos 168 (IRG, CAS# 31570-04-4), and 3: oxidized form of IRG (CAS# 95906-11-9).

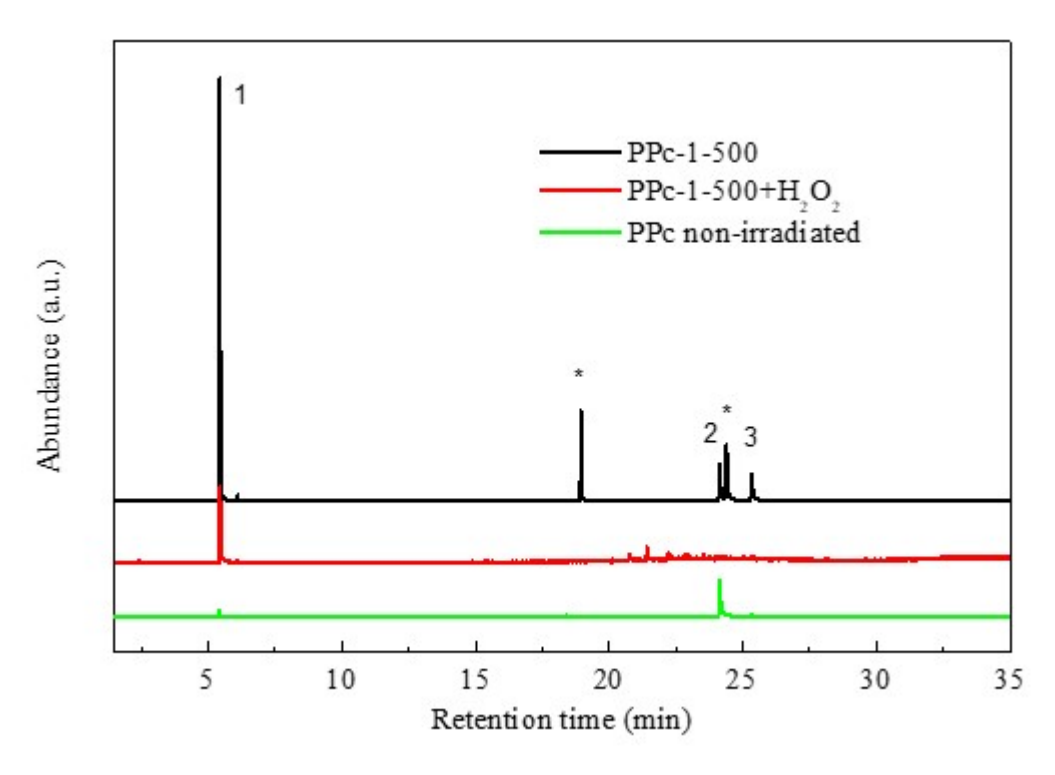


Figure S6: Ions with m/z 191 and 206 extracted from chromatograms acquired in SCAN mode in Figure S5. The numbers indicate IRG and its degradation products. 1: 2,4-di-tert-butylphenol (CAS# 96-76-4), 2: Irgafos 168 (IRG, CAS# 31570-04-4), and 3: oxidized form of IRG (CAS# 95906-11-9). The asterisk indicates other structures related to IRG.

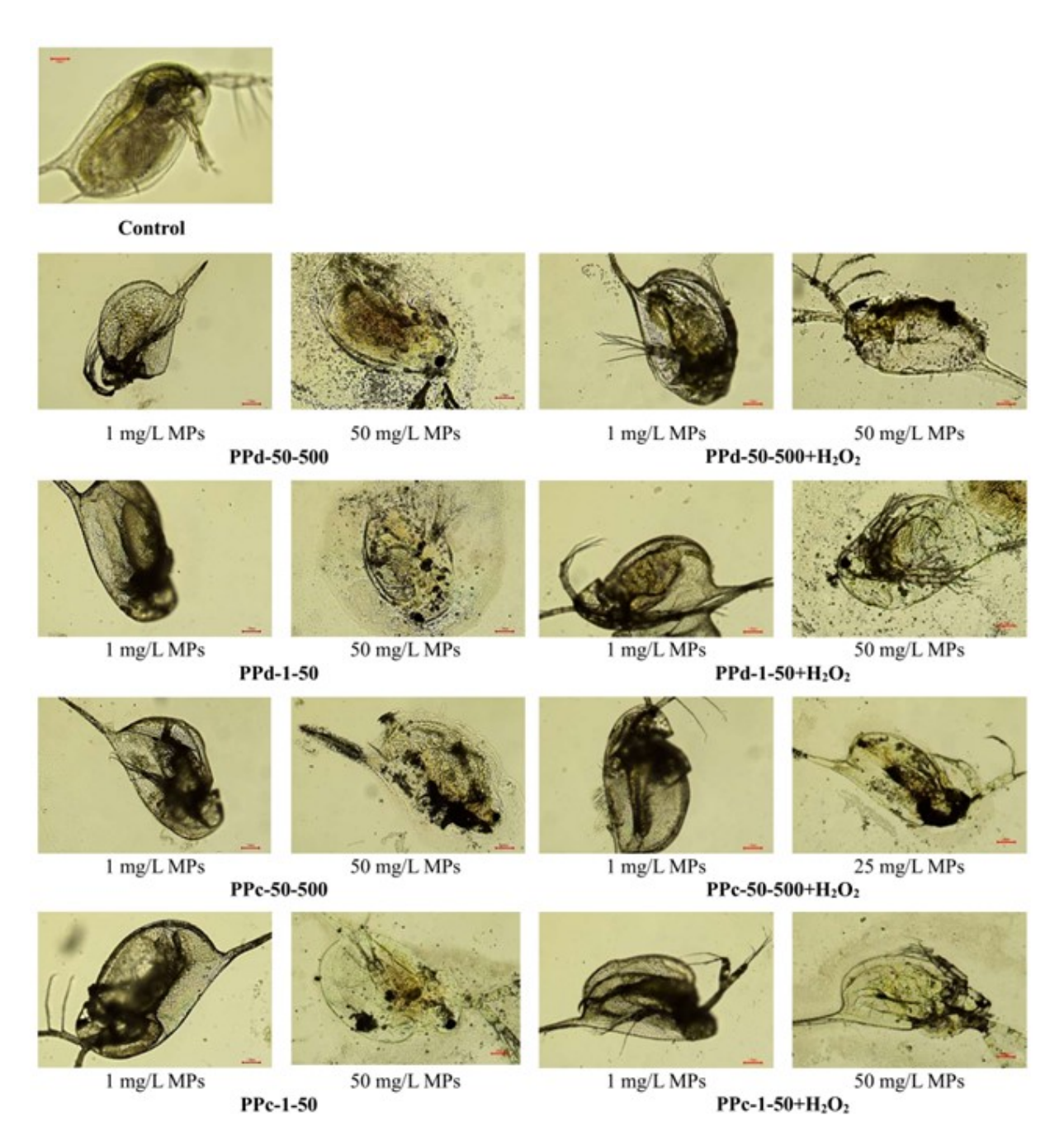


Figure S7: Optical micrographs corresponding to D. magna immobilization upon 48 h exposure to the MPs tested in this work (50-500 μ m and 1-50 μ m). PPc: commercial PP containing IRG and PPO, PPd: additive-free PP, 50-500: MPs within 50-500 μ m size range generated without H_2O_2 , $50-500+H_2O_2$: MPs within 50-500 μ m size range generated with H_2O_2 , 1-50: MPs within 1-50 μ m size range generated without H_2O_2 , $1-50+H_2O_2$: MPs within 1-50 μ m size range generated with H_2O_2 . IRG: Irgafos-168 additive, PPO: PP oligomers.

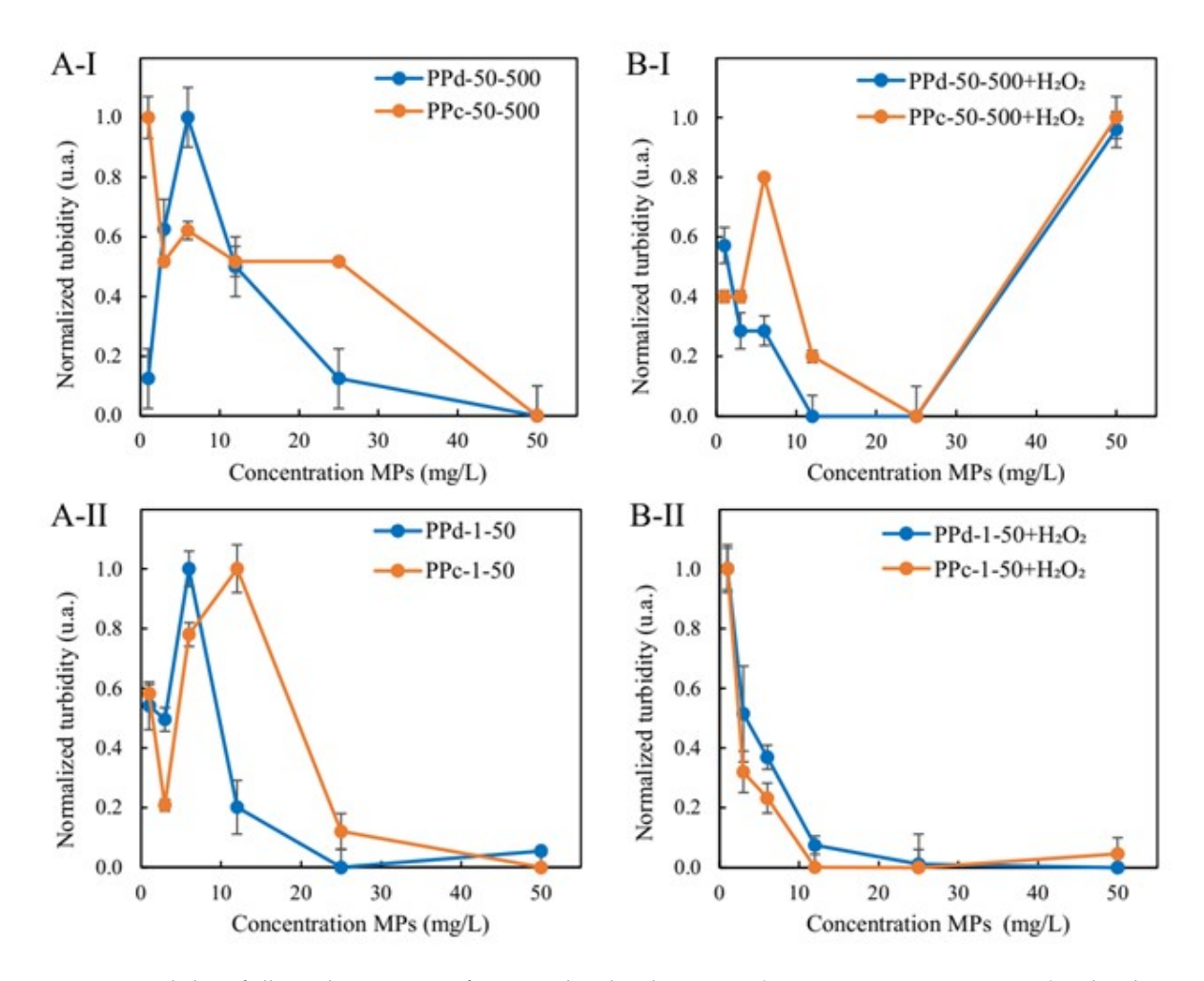


Figure S8: Turbidity of all tested suspensions of MPs irradiated without H_2O_2 (A-I: 50-500 μ m; A-II: 1-50 μ m) and with H_2O_2 (B-I: 50-500 μ m; B-II: 1-50 μ m), in R. subcapitata algae growth medium after 72 h of abiotic incubation. Error bars represent standard deviation. PPc: commercial PP containing IRG and PPO, PPd: additive-free PP, 50-500: MPs within 50-500 μ m size range generated without H_2O_2 , 50-500+ H_2O_2 : MPs within 50-500 μ m size range generated with H_2O_2 , 1-50: MPs within 1-50 μ m size range generated without H_2O_2 , 1-50+ H_2O_2 : MPs within 1-50 μ m size range generated with H_2O_2 . IRG: Irgafos-168 additive, PPO: PP oligomers.

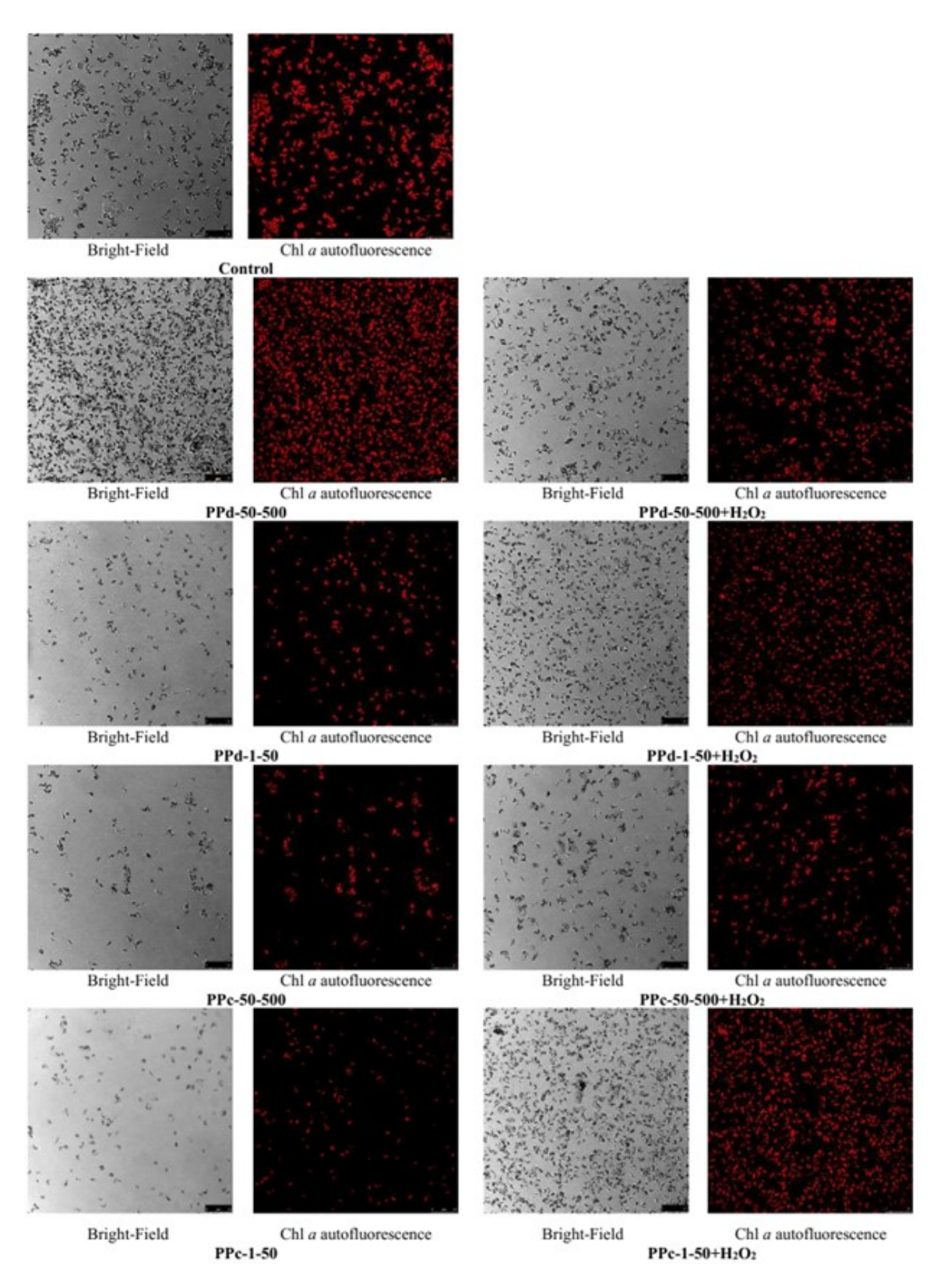


Figure S9: Confocal micrographs (Bright-Field and Chl a (λ_{ex} . 488 nm, λ_{em} . 595-700 nm) corresponding to growth rate of R. subcapitata upon 72 h exposure to a concentration of 3 mg/L of all MPs tested in this work. PPc: commercial PP containing IRG and PPO, PPd: additive-free PP, 50-500: MPs within 50-500 μ m size range generated without H_2O_2 , 50-500+ H_2O_2 : MPs within 50-500 μ m size range generated with H_2O_2 , 1-50: MPs within 1-50 μ m size range generated with H_2O_2 , 1-50+ H_2O_2 : MPs within 1-50 μ m size range generated with H_2O_2 . IRG: Irgafos-168 additive, PPO: PP oligomers.

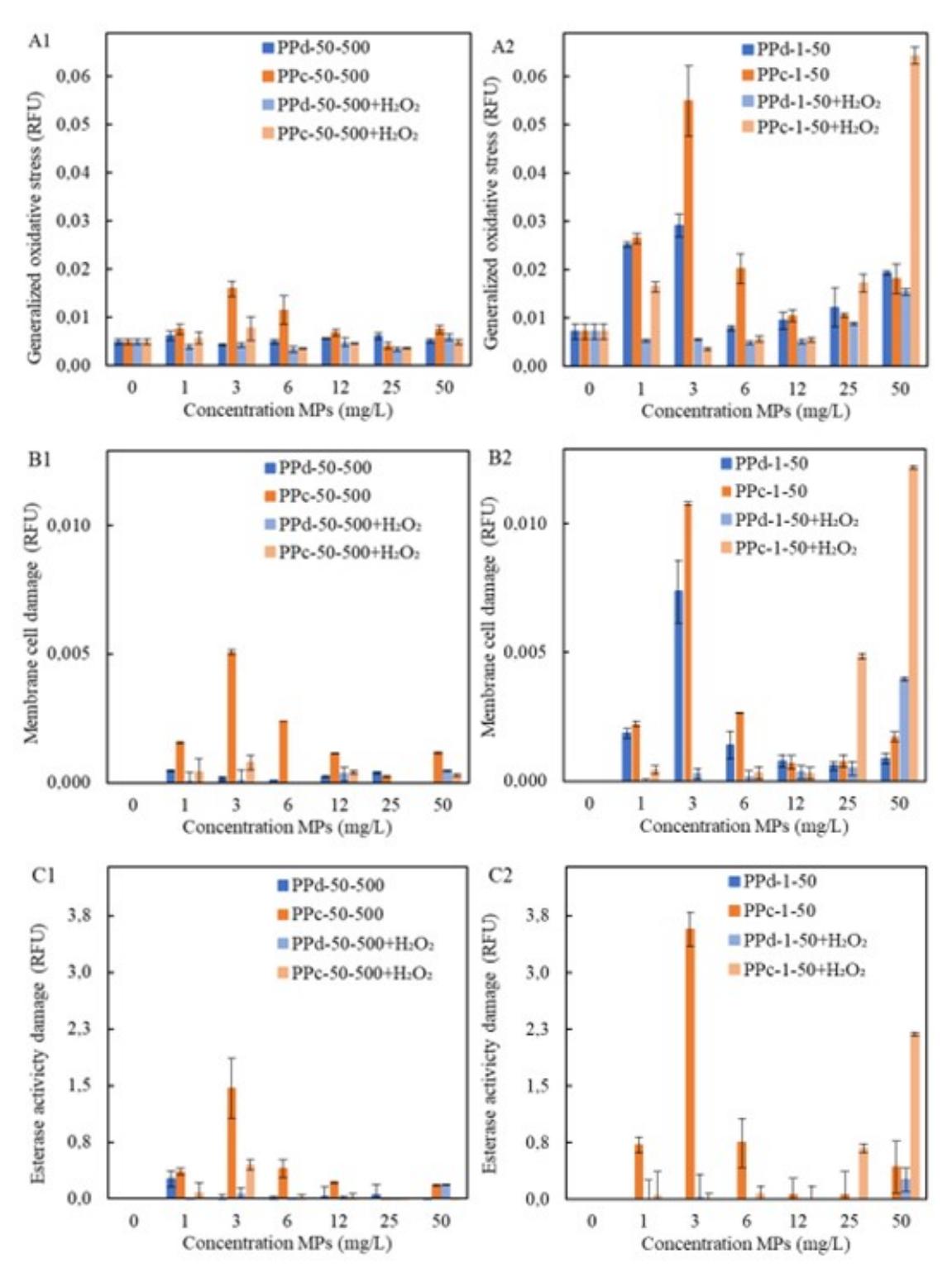


Figure S10: Alterations on relevant parameters of R. subcapitata after 72 h of exposure to all MPs generated in this work: (A) generalized oxidative stress; (B) membrane integrity; (C) metabolic- esterase activity. A1, B1, C1 (50-500 μ m) and A2, B2, C2 (1-50 μ m). Results are shown as RFU normalized with respect to the percentage of algal growth. Error bars represent the standard deviation. PPc: commercial PP containing IRG and PPO, PPd: additive-free PP, 50-500: MPs within 50-500 μ m size range generated without H_2O_2 , H_2O_2 : MPs within 50-500 μ m size range generated with H_2O_2 , H_2O_2 : MPs within 1-50 μ m size range generated with H_2O_2 . IRG: Irgafos-168 additive, PPO: PP oligomers.

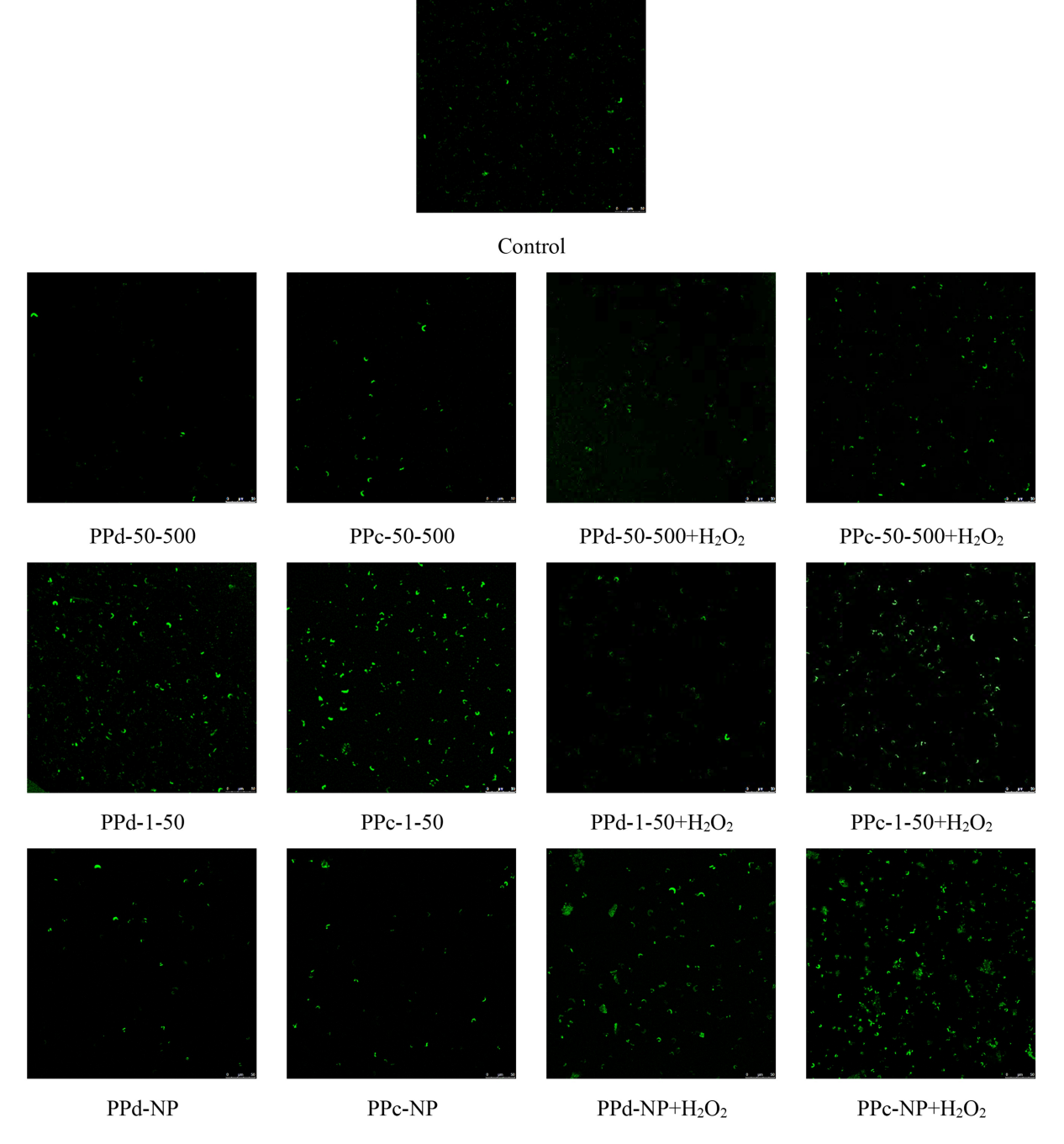


Figure S11: Confocal micrographs corresponding to generalized oxidative stress, ROS, produced on R. subcapitata upon 72 h exposure to a concentration of 1 mg/L of all MPs and NPs tested in this work. PPc: commercial PP containing IRG and PPO, PPd: additive-free PP, 50-500: MPs within 50-500 μ m size range generated without H_2O_2 , 50-500+ H_2O_2 : MPs within 50-500 μ m size range generated with H_2O_2 , 1-50: MPs within 1-50 μ m size range generated without H_2O_2 , 1-50+ H_2O_2 : MPs within 1-50 μ m size range generated with H_2O_2 , NP: NPs (< 1 μ m) generated with H_2O_2 , IRG: Irgafos-168 additive, PPO: PP oligomers.

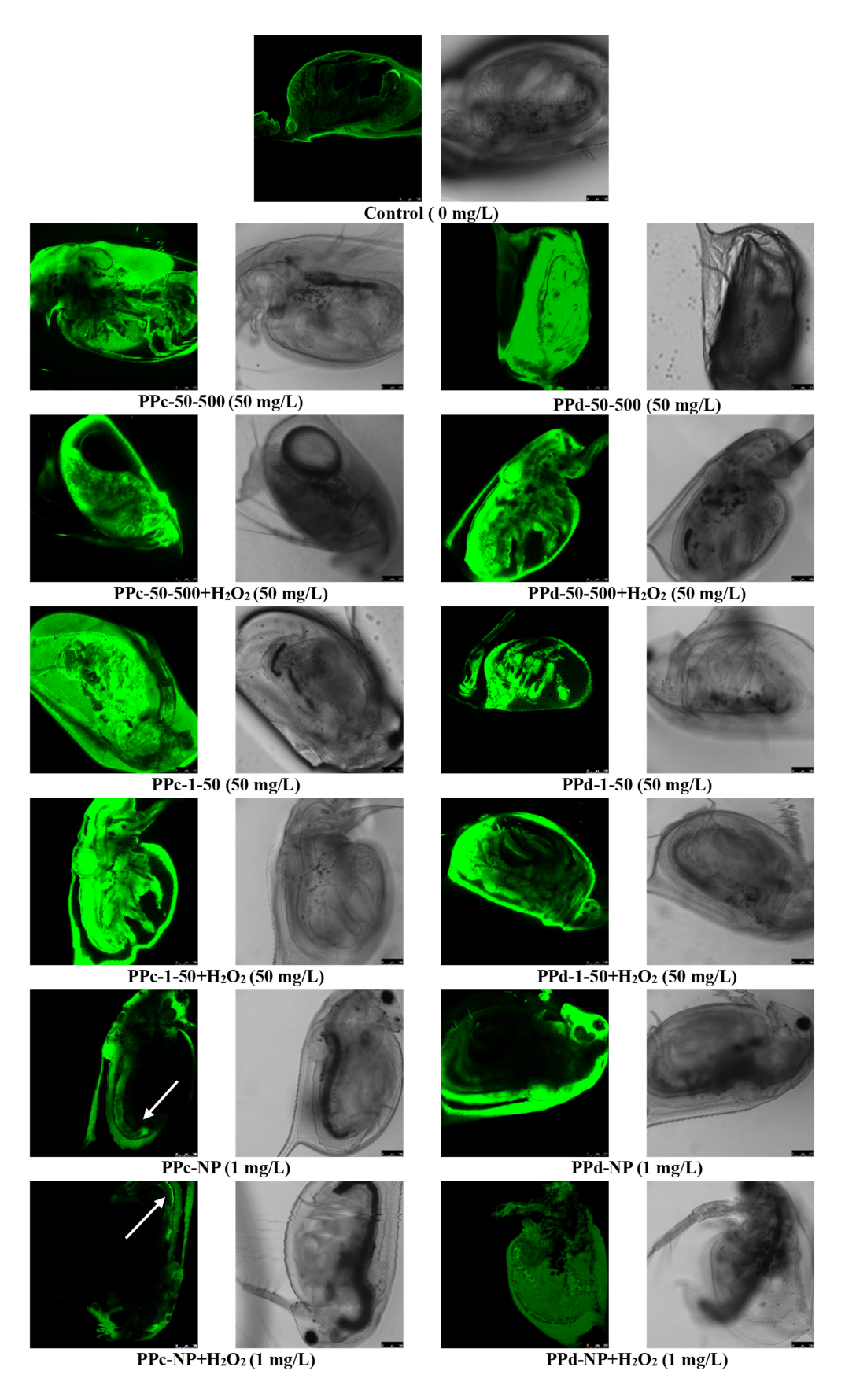


Figure S12: Confocal micrographs corresponding to generalized oxidative stress, ROS, status on D. magna upon 72 h exposure to a concentration of 50 mg/L of PPd and PPc MPs (within 1-50 μ m and 50-500 μ m size ranges) and 1 mg/L PPd and PPc NPs UV-generated, without and with H_2O_2 , respectively. PPc: commercial PP containing IRG and PPO, PPd: additive-free polypropylene. IRG: Irgafos-168 additive, PPO: PP oligomers.

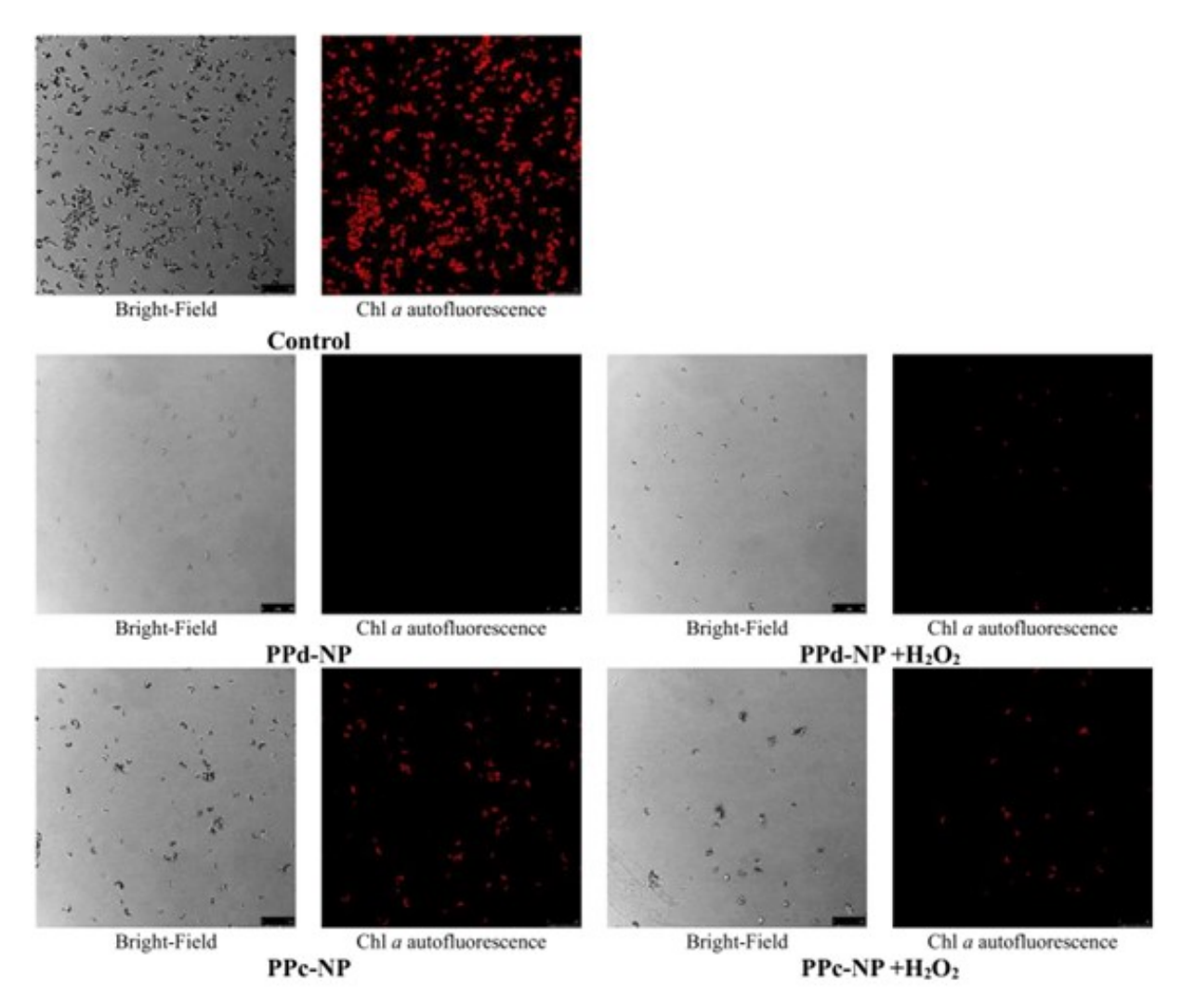


Figure S13: Confocal micrographs (Bright-Field and Chl a (λ_{ex} . 488 nm, λ_{em} . 595-700 nm) corresponding to growth rate of R. subcapitata upon 72 h exposure to 3 mg/l of all NPs tested in this work. PPc: commercial PP containing IRG and PPO, PPd: additive-free PP; NP: NPs (< 1 μ m) generated without H_2O_2 , NP+ H_2O_2 : NPs (< 1 μ m) generated with H_2O_2 . IRG: Irgafos-168 additive, PPO: PP oligomers.

Analyses of statistical significance. Pairwise comparison between treatments. Shadowed cells represent significant differences (p < 0.05).

A (R. subcapitata)

3 mg/L, no H ₂ O ₂	IRG	EXT	PPO	PPd-NP	PPd-NP-IRG	PPd-NP-EXT	PPd-NP-PPO	PPc-NP
IRG	_							
EXT		_						
PPO			_					
PPd-NP			0	_				
PPd-NP-IRG			-	4	-			1
PPd-NP-EXT						-		1 4
PPd-NP-PPO		_	_	_			-	
PPc-NP								-
7	10.5	FLOT	200	20110	201 NO 100	DD 4 ND FVT	201 112 222	00- ND
7 mg/L, no H ₂ O ₂	IRG	EXT	PPO	PPd-NP	PPd-NP-IRG	PPd-NP-EXT	PPd-NP-PPO	PPc-NP
IRG		_	-				-	
EXT		-						_
PPO						_		
PPd-NP		_	_	_			-	
PPd-NP-IRG								$\overline{}$
PPd-NP-EXT						-		
PPd-NP-PPO							-	
PPc-NP			3					
23 mg/L, no H ₂ O ₂	IRG	EXT	PPO	PPd-NP	PPd-NP-IRG	PPd-NP-EXT	PPd-NP-PPO	PPc-NP
IRG	_							
EXT		_						
PPO	1		_	1				
PPd-NP				-				
PPd-NP-IRG			_		-			
PPd-NP-EXT		+		_		-		
PPd-NP-PPO		-	_			_	_	
		_	_	_		_	_	-
PPc-NP								_
3 mg/L, H ₂ O ₂	IRG	EXT	PPO	PPd-NP	PPd-NP-IRG	PPd-NP-EXT	PPd-NP-PPO	PPc-NP
IRG	_							
	_	_	_	_			_	
EXT		-						
PPO PPO		-	-					
		-	-	_				
PPO		-	-	-	-			
PPO PPd-NP		-	-	-	-			
PPO PPd-NP PPd-NP-IRG		-	-	-	-	_	_	
PPO PPd-NP PPd-NP-IRG PPd-NP-EXT		-	-	-	-		-	-
PPO PPd-NP PPd-NP-IRG PPd-NP-EXT PPd-NP-PPO PPc-NP								- PDc.ND
PPO PPd-NP PPd-NP-IRG PPd-NP-EXT PPd-NP-PPO PPc-NP 7 mg/L, H ₂ O ₂	IRG	EXT	- PPO	PPd-NP	PPd-NP-IRG	PPd-NP-EXT	PPd-NP-PPO	
PPO PPd-NP PPd-NP-IRG PPd-NP-EXT PPd-NP-PPO PPc-NP 7 mg/L, H ₂ O ₂ IRG		EXT						
PPO PPd-NP PPd-NP-IRG PPd-NP-EXT PPd-NP-PPO PPc-NP 7 mg/L, H ₂ O ₂ IRG EXT	IRG		PPO					
PPO PPd-NP PPd-NP-IRG PPd-NP-EXT PPd-NP-PPO PPc-NP 7 mg/L, H ₂ O ₂ IRG EXT PPO	IRG	EXT		PPd-NP				
PPO PPd-NP PPd-NP-IRG PPd-NP-EXT PPd-NP-PPO PPc-NP 7 mg/L, H ₂ O ₂ IRG EXT PPO PPd-NP	IRG	EXT	PPO		PPd-NP-IRG			PPc-NP
PPO PPd-NP PPd-NP-IRG PPd-NP-EXT PPd-NP-PPO PPc-NP 7 mg/L, H ₂ O ₂ IRG EXT PPO PPd-NP PPd-NP-IRG	IRG	EXT	PPO	PPd-NP		PPd-NP-EXT		PPc-NP
PPO PPd-NP PPd-NP-IRG PPd-NP-EXT PPd-NP-PPO PPc-NP 7 mg/L, H ₂ O ₂ IRG EXT PPO PPd-NP PPd-NP-IRG PPd-NP-EXT	IRG	EXT	PPO	PPd-NP	PPd-NP-IRG		PPd-NP-PPO	PPc-NP
PPO PPd-NP PPd-NP-IRG PPd-NP-EXT PPd-NP-PPO PPc-NP 7 mg/L, H ₂ O ₂ IRG EXT PPO PPd-NP PPd-NP-IRG PPd-NP-EXT PPd-NP-EXT	IRG	EXT	PPO	PPd-NP	PPd-NP-IRG	PPd-NP-EXT		
PPO PPd-NP PPd-NP-IRG PPd-NP-EXT PPd-NP-PPO PPc-NP 7 mg/L, H ₂ O ₂ IRG EXT PPO PPd-NP PPd-NP-IRG PPd-NP-EXT	IRG	EXT	PPO	PPd-NP	PPd-NP-IRG	PPd-NP-EXT	PPd-NP-PPO	PPc-NP
PPO PPd-NP PPd-NP-IRG PPd-NP-EXT PPd-NP-PPO PPc-NP 7 mg/L, H ₂ O ₂ IRG EXT PPO PPd-NP PPd-NP-IRG PPd-NP-EXT PPd-NP-EXT	IRG	EXT	PPO	PPd-NP	PPd-NP-IRG	PPd-NP-EXT	PPd-NP-PPO	
PPO PPd-NP PPd-NP-IRG PPd-NP-EXT PPd-NP-PPO PPc-NP 7 mg/L, H ₂ O ₂ IRG EXT PPO PPd-NP PPd-NP-IRG PPd-NP-IRG PPd-NP-EXT PPd-NP-EXT PPd-NP-PPO PPc-NP	IRG	EXT	PPO —	PPd-NP	PPd-NP-IRG	PPd-NP-EXT	PPd-NP-PPO	_
PPO PPd-NP PPd-NP-IRG PPd-NP-EXT PPd-NP-PPO PPc-NP 7 mg/L, H ₂ O ₂ IRG EXT PPO PPd-NP PPd-NP-IRG PPd-NP-EXT PPd-NP-EXT PPd-NP-PPO PPc-NP 23 mg/L, H ₂ O ₂	IRG	EXT	PPO —	PPd-NP	PPd-NP-IRG	PPd-NP-EXT	PPd-NP-PPO	_
PPO PPd-NP PPd-NP-IRG PPd-NP-EXT PPd-NP-PPO PPc-NP 7 mg/L, H ₂ O ₂ IRG EXT PPO PPd-NP PPd-NP-IRG PPd-NP-IRG PPd-NP-EXT PPd-NP-PPO PPc-NP 23 mg/L, H ₂ O ₂ IRG	IRG	EXT —	PPO —	PPd-NP	PPd-NP-IRG	PPd-NP-EXT	PPd-NP-PPO	_
PPO PPd-NP PPd-NP-IRG PPd-NP-EXT PPd-NP-PPO PPc-NP 7 mg/L, H ₂ O ₂ IRG EXT PPO PPd-NP PPd-NP-IRG PPd-NP-EXT PPd-NP-EXT PPd-NP-EXT PPd-NP-PPO PPc-NP 23 mg/L, H ₂ O ₂ IRG EXT	IRG	EXT —	PPO PPO	PPd-NP	PPd-NP-IRG	PPd-NP-EXT	PPd-NP-PPO	_
PPO PPd-NP PPd-NP-IRG PPd-NP-EXT PPd-NP-PPO PPc-NP 7 mg/L, H ₂ O ₂ IRG EXT PPO PPd-NP-IRG PPd-NP-IRG PPd-NP-EXT PPd-NP-PPO PPc-NP 23 mg/L, H ₂ O ₂ IRG EXT PPO PPC-NP	IRG	EXT —	PPO PPO	PPd-NP	PPd-NP-IRG	PPd-NP-EXT	PPd-NP-PPO	_
PPO PPd-NP PPd-NP-IRG PPd-NP-EXT PPd-NP-PPO PPc-NP 7 mg/L, H ₂ O ₂ IRG EXT PPO PPd-NP-IRG PPd-NP-IRG PPd-NP-EXT PPd-NP-PPO PPc-NP 23 mg/L, H ₂ O ₂ IRG EXT PPO PPd-NP-IRG PPd-NP-IRG PPd-NP-IRG	IRG	EXT —	PPO PPO	PPd-NP	PPd-NP-IRG	PPd-NP-EXT	PPd-NP-PPO	_
PPO PPd-NP PPd-NP-IRG PPd-NP-EXT PPd-NP-PPO PPc-NP 7 mg/L, H ₂ O ₂ IRG EXT PPO PPd-NP-IRG PPd-NP-IRG PPd-NP-PPO PPc-NP 23 mg/L, H ₂ O ₂ IRG EXT PPO PPd-NP-IRG PPd-NP-IRG PPd-NP-IRG PPd-NP-IRG PPd-NP-IRG PPd-NP-IRG	IRG	EXT —	PPO PPO	PPd-NP	PPd-NP-IRG	PPd-NP-EXT	PPd-NP-PPO PPd-NP-PPO	_
PPO PPd-NP PPd-NP-IRG PPd-NP-EXT PPd-NP-PPO PPc-NP 7 mg/L, H ₂ O ₂ IRG EXT PPO PPd-NP-IRG PPd-NP-IRG PPd-NP-EXT PPd-NP-PPO PPc-NP 23 mg/L, H ₂ O ₂ IRG EXT PPO PPd-NP-IRG PPd-NP-IRG PPd-NP-IRG	IRG	EXT —	PPO PPO	PPd-NP	PPd-NP-IRG	PPd-NP-EXT	PPd-NP-PPO	_

B (D. magna)

3 mg/L, no H ₂ O ₂	IRG	EXT	PPO	PPd-NP	PPd-NP-IRG	PPd-NP-EXT	PPd-NP-PPO	PPc-NP
IRG	_							
EXT		_						
PPO			-					
PPd-NP				_				
PPd-NP-IRG					-			
PPd-NP-EXT						_		
PPd-NP-PPO							_	
PPc-NP								_
rre-w	- C							
7 mg/L, no H ₂ O ₂	IRG	EXT	PPO	PPd-NP	PPd-NP-IRG	PPd-NP-EXT	PPd-NP-PPO	PPc-NP
IRG	_				4			
EXT		-						
PPO	S		-					
PPd-NP								
PPd-NP-IRG					-			
PPd-NP-EXT	à I					-		
PPd-NP-PPO								
PPc-NP								
	100	EVT	200	004 NO	and his inc	004 NO EVE	004 NO 000	DD+ ND
23 mg/L, no H ₂ O ₂	IRG	EXT	PPO	PPd-NP	PPd-NP-IRG	PPO-NP-EXT	PPd-NP-PPO	PPC-NP
IRG		10000						
EXT	-	-		_				
PPO	-	_	-	-				
PPd-NP			1.7	_				
PPd-NP-IRG				-	-			
PPd-NP-EXT				-	_	_		
PPd-NP-PPO							-	
PPc-NP								1
			_					_
3 mg/L, H ₂ O ₂	IRG	EXT	PPO	PPd-NP	PPd-NP-IRG	PPd-NP-EXT	PPd-NP-PPO	PPc-NP
3 mg/L, H ₂ O ₂ IRG	IRG _	EXT	PPO	PPd-NP	PPd-NP-IRG	PPd-NP-EXT	PPd-NP-PPO	Alamana and a
		EXT —	PPO	PPd-NP	PPd-NP-IRG	PPd-NP-EXT	PPd-NP-PPO	Alamana and a
IRG			PPO	PPd-NP	PPd-NP-IRG	PPd-NP-EXT	PPd-NP-PPO	Alamana and a
IRG EXT				PPd-NP	PPd-NP-IRG	PPd-NP-EXT	PPd-NP-PPO	Alamana and a
IRG EXT PPO				12	PPd-NP-IRG	PPd-NP-EXT	PPd-NP-PPO	Alamana and a
IRG EXT PPO PPd-NP				12		PPd-NP-EXT	PPd-NP-PPO	Alamana and a
IRG EXT PPO PPd-NP PPd-NP-IRG				12				Alamana and a
IRG EXT PPO PPd-NP PPd-NP-IRG PPd-NP-EXT PPd-NP-PPO				12			PPd-NP-PPO	PPc-NP
IRG EXT PPO PPd-NP PPd-NP-IRG PPd-NP-EXT PPd-NP-PPO PPc-NP	-	_	_	-	-	_	_	PPc-NP
IRG EXT PPO PPd-NP PPd-NP-IRG PPd-NP-EXT PPd-NP-PPO PPc-NP 7 mg/L, H ₂ O ₂	IRG			12			_	PPc-NP
IRG EXT PPO PPd-NP PPd-NP-IRG PPd-NP-EXT PPd-NP-PPO PPc-NP 7 mg/L, H ₂ O ₂ IRG	-	EXT	_	-	-	_	_	PPc-NP
IRG EXT PPO PPd-NP PPd-NP-IRG PPd-NP-EXT PPd-NP-PPO PPc-NP 7 mg/L, H ₂ O ₂ IRG EXT	IRG	_	PPO	-	-	_	_	PPc-NP
IRG EXT PPO PPd-NP PPd-NP-IRG PPd-NP-EXT PPd-NP-PPO PPc-NP 7 mg/L, H ₂ O ₂ IRG EXT PPO	IRG	EXT	_	PPd-NP	-	_	_	PPc-NP
IRG EXT PPO PPd-NP PPd-NP-IRG PPd-NP-EXT PPd-NP-PPO PPc-NP 7 mg/L, H ₂ O ₂ IRG EXT PPO PPd-NP	IRG	EXT	PPO	-	PPd-NP-IRG	_	_	PPc-NP
IRG EXT PPO PPd-NP PPd-NP-IRG PPd-NP-EXT PPd-NP-PPO PPc-NP 7 mg/L, H ₂ O ₂ IRG EXT PPO PPd-NP PPd-NP	IRG	EXT	PPO	PPd-NP	-	PPd-NP-EXT	_	PPc-NP
IRG EXT PPO PPd-NP PPd-NP-IRG PPd-NP-EXT PPd-NP-PPO PPc-NP 7 mg/L, H ₂ O ₂ IRG EXT PPO PPd-NP PPd-NP-IRG PPd-NP-EXT	IRG	EXT	PPO	PPd-NP	PPd-NP-IRG	_	PPd-NP-PPO	PPc-NP
IRG EXT PPO PPd-NP PPd-NP-IRG PPd-NP-EXT PPd-NP-PPO PPc-NP 7 mg/L, H ₂ O ₂ IRG EXT PPO PPd-NP PPd-NP-IRG PPd-NP-EXT PPd-NP-EXT	IRG	EXT	PPO	PPd-NP	PPd-NP-IRG	PPd-NP-EXT	_	PPc-NP PPc-NP
IRG EXT PPO PPd-NP PPd-NP-IRG PPd-NP-EXT PPd-NP-PPO PPc-NP 7 mg/L, H ₂ O ₂ IRG EXT PPO PPd-NP PPd-NP-IRG PPd-NP-EXT	IRG	EXT	PPO	PPd-NP	PPd-NP-IRG	PPd-NP-EXT	PPd-NP-PPO	PPc-NP
IRG EXT PPO PPd-NP PPd-NP-IRG PPd-NP-EXT PPd-NP-PPO PPc-NP 7 mg/L, H ₂ O ₂ IRG EXT PPO PPd-NP PPd-NP-IRG PPd-NP-EXT PPd-NP-EXT	IRG	EXT	PPO	PPd-NP	PPd-NP-IRG	PPd-NP-EXT	PPd-NP-PPO	PPc-NP PPc-NP
IRG EXT PPO PPd-NP PPd-NP-IRG PPd-NP-EXT PPd-NP-PPO PPc-NP 7 mg/L, H₂O₂ IRG EXT PPO PPd-NP PPd-NP PPd-NP-IRG PPd-NP-EXT PPd-NP-EXT PPd-NP-PPO PPc-NP	IRG	EXT —	PPO —	PPd-NP	PPd-NP-IRG	PPd-NP-EXT	PPd-NP-PPO	PPc-NP PPc-NP
IRG EXT PPO PPd-NP PPd-NP-IRG PPd-NP-EXT PPd-NP-PPO PPc-NP 7 mg/L, H ₂ O ₂ IRG EXT PPO PPd-NP PPd-NP-IRG PPd-NP-IRG PPd-NP-EXT PPd-NP-EXT PPd-NP-EXT PPd-NP-PPO PPc-NP 23 mg/L, H ₂ O ₂	IRG —	EXT —	PPO —	PPd-NP	PPd-NP-IRG	PPd-NP-EXT	PPd-NP-PPO	PPc-NP PPc-NP
IRG EXT PPO PPd-NP PPd-NP-IRG PPd-NP-EXT PPd-NP-PPO PPc-NP 7 mg/L, H ₂ O ₂ IRG EXT PPO PPd-NP PPd-NP-IRG PPd-NP-EXT PPd-NP-EXT PPd-NP-EXT PPd-NP-EXT PPd-NP-PPO PPc-NP 23 mg/L, H ₂ O ₂ IRG	IRG —	EXT —	PPO —	PPd-NP	PPd-NP-IRG	PPd-NP-EXT	PPd-NP-PPO	PPc-NP PPc-NP
IRG EXT PPO PPd-NP PPd-NP-IRG PPd-NP-EXT PPd-NP-PPO PPc-NP 7 mg/L, H ₂ O ₂ IRG EXT PPO PPd-NP-IRG PPd-NP-EXT PPd-NP-EXT PPd-NP-EXT PPd-NP-EXT PPd-NP-PPO PPc-NP 23 mg/L, H ₂ O ₂ IRG EXT	IRG —	EXT —	PPO PPO	PPd-NP	PPd-NP-IRG	PPd-NP-EXT	PPd-NP-PPO	PPc-NP PPc-NP
IRG EXT PPO PPd-NP PPd-NP-IRG PPd-NP-EXT PPd-NP-PPO PPc-NP 7 mg/L, H ₂ O ₂ IRG EXT PPO PPd-NP-IRG PPd-NP-IRG PPd-NP-EXT PPd-NP-PPO PPc-NP 23 mg/L, H ₂ O ₂ IRG EXT	IRG —	EXT —	PPO PPO	PPd-NP	PPd-NP-IRG	PPd-NP-EXT	PPd-NP-PPO	PPc-NP PPc-NP
IRG EXT PPO PPd-NP PPd-NP-IRG PPd-NP-EXT PPd-NP-PPO PPc-NP 7 mg/L, H ₂ O ₂ IRG EXT PPO PPd-NP-IRG PPd-NP-IRG PPd-NP-EXT PPd-NP-EXT PPd-NP-PPO PPc-NP 23 mg/L, H ₂ O ₂ IRG EXT PPO PPc-NP	IRG —	EXT —	PPO PPO	PPd-NP	PPd-NP-IRG	PPd-NP-EXT	PPd-NP-PPO	PPc-NP PPc-NP
IRG EXT PPO PPd-NP PPd-NP-IRG PPd-NP-EXT PPd-NP-PPO PPc-NP 7 mg/L, H ₂ O ₂ IRG EXT PPO PPd-NP-IRG PPd-NP-EXT PPd-NP-EXT PPd-NP-PPO PPc-NP 23 mg/L, H ₂ O ₂ IRG EXT PPO PPd-NP-PPO PPc-NP	IRG —	EXT —	PPO PPO	PPd-NP	PPd-NP-IRG	PPd-NP-EXT PPd-NP-EXT	PPd-NP-PPO	PPc-NP PPc-NP
IRG EXT PPO PPd-NP PPd-NP-IRG PPd-NP-EXT PPd-NP-PPO PPc-NP 7 mg/L, H ₂ O ₂ IRG EXT PPO PPd-NP-IRG PPd-NP-EXT PPd-NP-EXT PPd-NP-EXT PPd-NP-PPO PPc-NP 23 mg/L, H ₂ O ₂ IRG EXT PPO PPd-NP-PPO PPc-NP	IRG —	EXT —	PPO PPO	PPd-NP	PPd-NP-IRG	PPd-NP-EXT PPd-NP-EXT	PPd-NP-PPO PPd-NP-PPO	PPc-NP PPc-NP

ANCOVA statistical analyses. For R. subcapitata (A) and D. magna (B). IRG and H_2O_2 are categorical variables. Size (taken from Table 1) and concentrations are continuous variables.

```
A
                           Df Sum Sq Mean Sq F value
                                     340 340.0 6.149 0.013465 *
                                     1244 1244.5 22.504 2.71e-06 ***
size 1 711 711.4 12.865 0.000366 ***
conc. 1 1985 1985.0 35.895 3.88e-09 ***
IRG:H202 1 49 49.0 0.887 0.346845
IRG:size 1 205 204.9 3.705 0.054803 .
IRG:size 1 205 204.9 3.703 0.054803 .

IRG:conc. 1 24 24.5 0.442 0.506222

H202:size 1 756 755.7 13.665 0.000242 ***

H202:conc. 1 206 205.9 3.723 0.054198 .

size:conc. 1 787 786.8 14.229 0.000180 ***

Residuals 523 28922 55.3
 '***', p < 0.001; '**' p < 0.01; '*' p < 0.05; '.' p < 0.1
                           Df Sum Sq Mean Sq F value
                                                                                  Pr (>F)
                           1 1711 1711 7.260 0.007636 **
 IRG
H202
                                     169
                                                     169 0.717 0.397976
H2O2 1 169 169 0.717 0.397976
size 1 4215 4215 17.885 3.54e-05 ***
conc. 1 7845 7845 33.291 2.92e-08 ***
IRG:H2O2 1 3 3 0.013 0.909917
IRG:size 1 1641 1641 6.964 0.008957 **
IRG:conc. 1 598 598 2.535 0.112862
H2O2:size 1 3803 3803 16.137 8.28e-05 ***
H2O2:conc. 1 7 7 0.032 0.858808
size:conc. 1 2817 2817 11.955 0.000663 ***
Residuals 204 48074
                                                     236
 '***', p < 0.001; '**' p < 0.01; '*' p < 0.05; '.' p < 0.1
```